



1 Manuscript type: Research article

## 2 **Assessing Landslide Damming susceptibility in Central Asia**

3 Carlo Tacconi Stefanelli<sup>a,b,\*</sup>, William Frodella<sup>a,b</sup>, Francesco Caleca<sup>a,b</sup>, Zhanar Raimbekova<sup>c</sup>,  
4 Ruslan Umuraliev<sup>d</sup>, Veronica Tofani<sup>a,b</sup>

5 <sup>a</sup> University of Florence, Department of Earth Sciences, via G. la Pira 4, 50121 Florence, Italy

6 <sup>b</sup> UNESCO Chair on the Prevention and Sustainable Management of Geo-Hydrological Hazards, University of  
7 Florence, Largo Fermi 2, 50125 Florence, Italy

8 <sup>c</sup> Institute of Seismology of Republic of Kazakhstan (IS), Almaty, Kazakhstan

9 <sup>d</sup> Institute of Seismology of the National Academy of Sciences of Kyrgyz Republic (ISNASKR), Bishkek, Kyrgyz  
10 Republic

11 \* Correspondence to: carlo.tacconistefanelli@unifi.it

### 12 **Abstract**

13 Central Asia regions are characterized by active tectonics, high mountain chains with extreme topography with  
14 glaciers and strong seasonal rainfall events. These key predisposing factors make large landslides a serious natural  
15 threat in the area, causing several casualties every year. The mountain crests are divided by wide lenticular or  
16 narrow, linear intermountain tectonic depressions, which are incised by many of the most important Central Asia  
17 rivers and are also subject to major seasonal river flood hazard. This multi-hazard combination is a source of  
18 potential damming scenarios which can bring cascading effects with devastating consequences for the surrounding  
19 settlements and population. Different hazards can only be managed with a multi-hazard approach coherent within  
20 the different countries, as suggested by the requirements of the Sendai Framework for Disaster Risk Reduction.

21 This work was carried out within the framework of the SFRARR Project (“*Strengthening Financial Resilience  
22 and Accelerating Risk Reduction in Central Asia*”) as a part of a multi-hazard approach with the aim of providing  
23 a damming susceptibility analysis at a regional scale for Central Asia. To achieve this, a semi-automated GIS-  
24 based mapping method, centred on a bivariate correlation of morphometric parameters defined by a morphological  
25 index, originally designed to assess the damming susceptibility at basin/regional scale, was modified to be adopted  
26 nationwide and applied to spatially assess the obstruction of the river network in Central Asia for mapped and  
27 newly formed landslides. The proposed methodology represents an improvement of the previously designed,  
28 requiring a smaller amount of data, bringing new information on the damming hazard management and risk  
29 reduction for the Central Asia regions.

### 30 **1 Introduction**

31 The mountainous areas of the Djungaria, Tien Shan, Pamir and Kopetdag in Central Asia territories are  
32 characterized by complex and active tectonic and are the sources of most of Central Asia rivers. A rugged  
33 topography along with complex geological structure and high seismicity are ideal setting for large slope failures.  
34 In general, when landslides completely obstruct a river channel, they generate a landslide dam whose consequences



35 can be a serious hazard forming upstream backwater and causing catastrophic downstream flooding, changes in  
36 the riverbed course, embankments instability triggering other landslides with a cascading effect (Swanson et al.  
37 1986; Costa and Schuster 1988; Casagli and Ermini 1999). The effects of impounded water and anomalous flood  
38 waves, resulting from a dam breach, have significant economic and social impacts in upstream and downstream  
39 areas with economic and human losses (King et al. 1989; Dai et al. 2005; Chen and Chang 2016). Rebuilding costs  
40 can be extensive, as they are direct (e.g., infrastructure and buildings reconstruction, safety measures) and indirect  
41 (e.g., loss in real estate value and damage caused to industrial and agricultural production), harder to estimate.

42 Most of landslide dams have a short life as about 40% of them collapse within 24 hours after formation and about  
43 80% within one year (Tacconi Stefanelli et al, 2015; Fan et al., 2020). Given the limited available time, a complete  
44 and reliable analysis of the risks, requiring in-depth study of the phenomenon, is not achievable during the event  
45 and only rapid assessments for the dam stability are suitable. When the people to evacuate are too many or the  
46 related risk is too high, engineering measures for the hazard reduction are attempted: among these are for example  
47 modification of slope geometry, drainage, retaining structures and internal slope reinforcement (Popescu and  
48 Sasahara 2009; Schuster and Evans 2011). Therefore, part of the effects from landslide damming can be avoided  
49 or at least reduced thanks to mitigation and prevention measures (e.g., slopes stabilization or re-profiling) if the  
50 most critical areas with the highest damming probability are known. Consequently, planning and prevention tools,  
51 such as risk and susceptibility mapping, are essential to reduce the costs of natural hazard and improve the  
52 efficiency of environmental management.

53 Reactivation of ancient landslides triggered during different climatic and environmental conditions may often  
54 generate new mass movements (Casagli and Ermini 1999; Canuti et al. 2004; Dikau and Schrott 1999; Borgatti  
55 and Soldati 2010; Crozier 2010). Landslides generated in the past are now dormant, with strength parameters of  
56 the sliding surface close to the residual ones, and difficult to recognize because vegetation, erosion and superficial  
57 alteration hide their morphology. Natural causes, such as earthquakes, river undercutting, rainfall, and snowmelt,  
58 or even anthropic activity can reactivate these ancient phenomena. Therefore, all dormant landslides capable to  
59 reach a river along their pathway can potentially dam it and should be investigated. New landslides, instead, may  
60 develop wherever are present suitable conditions along the slopes. The spatial occurrence probability is commonly  
61 assessed by landslide susceptibility analysis, highly dependent on landslide volume (Catani et al., 2016), which is  
62 difficult to accurately predict.

63 Landslides in Central Asia are quite common and a considerable number of them have huge dimension, often  
64 induced by strong earthquakes but also by floods highly rainfall and snowmelt (Behling et al., 2014; Golovko,  
65 2015; Havenith et al., 2015a, 2015b, 2006b; Kalmatieva et al., 2009; Rosi et al., 2023; Saponaro et al., 2014; Strom  
66 and Abdrakhmatov, 2017, 2018). Concerning landslide dam events, in Central Asia regions several mass  
67 movements of considerable size produced the obstruction of a river section, of which more than 100 still are  
68 existing with a lake (Strom, 2010). Although many of these could be considered stable (Strom, 2010), the  
69 occurrence of devastating outburst floods in the last century show that their potential hazard should never be  
70 overlooked also considering the seismicity of the region. In the Rushan and Murgab districts of Gorno-Badakhshan  
71 Autonomous Oblast (Pamirs, Tajikistan) along the Murghab river, the Usoi dam is one of the most famous of the  
72 many cases in the regions. Its impounded lake, called Lake Sarez, is 60 km long with 500 m of depth and has a



73 stored volume of about  $17 \text{ km}^3$ , representing the world deepest landslide-dammed lake (Costa and Schuster, 1991;  
74 Fan et al., 2020). It was originated on February 18th, 1911, when a MW 7.2 earthquake triggered a giant wedge-  
75 failure of about  $2.2 \text{ km}^3$  of rock (mainly quartzite, schist, shale and dolomite) and debris that blocked the Murgab  
76 River and a tributary valley, forming the 560 m high, 5 km long and 4 km wide Usoi dam, impounding Lake Sarez,  
77 also creating the smaller Lake Shadau (Strom, 2010).

78 Landslide dam evolution, according to some studies (Swanson et al. 1986; Ermini and Casagli, 2003; Dal Sasso et  
79 al. 2014; Tacconi Stefanelli et al. 2016), can be estimated through geomorphological indexes which require  
80 parameters characterizing the landslide (or the dam) and the river (or the lake). Geomorphological indexes are a  
81 powerful classification tool, but their prediction power depend mainly on long studies, a large amount of data and  
82 measurement efforts given their empirical nature. Many of these indexes need parameters not always available and  
83 easy to acquire, such as grain size distribution (Liao et al. 2022) or landslide velocity (Swanson et al., 1986).

84 In this work, we propose a simple semi-automatic GIS-based mapping methodology to verify the damming  
85 susceptibility of river networks at national scale from existing and neo-formed landslides trough a  
86 geomorphological index. This activity research was carried out in the framework of the SFRARR Project  
87 (“*Strengthening Financial Resilience and Accelerating Risk Reduction in Central Asia*”) as a part of a multi-hazard  
88 approach (Bazzurro et al., 2023).

89 The proposed mapping methodology represents an innovation in terms of application simplicity, availability of  
90 data and of extension of the analysed area, bringing new information on the damming hazard in the Central Asia  
91 regions where the landslide susceptibility is quite high (Rosi et al., 2023) and a set of input data required for the  
92 methodology application were available.

## 93 **2 Study area**

94 Central Asia is a region of vast diversity encompassing high mountain chains, deserts, and steppes (Figure 1). The  
95 southern and eastern parts of the region are predominantly occupied by the mountainous areas of Djungaria, Tien  
96 Shan, Pamir, Kopetdag, and a small part of Western Altaj, with peaks exceeding 7,000 m above sea level (a.s.l.)  
97 (Strom, 2010). These intraplate mountain systems, developed in the Cenozoic as a result of the India-Asian  
98 collision, is located between the Tarim Basin and the Kazakh Shield (Molnar and Tapponier 1975, Abdrakhmatov  
99 et al., 1996; 2003; Zubovich et al., 2010, Ullah et al., 2015). This study focuses the attention on the territories of  
100 Central Asia that includes Turkmenistan, Kazakhstan, Kyrgyz Republic, Uzbekistan, and Tajikistan, covering a  
101 surface of more than  $4 \cdot 10^6 \text{ km}^2$ . Mountain building began in the Oligocene (Chedia 1980) or later (Abdrakhmatov  
102 et al. 1996), resulting in a complex system of basement folds interrupted by several thrusts and reverse faults with  
103 lateral offset of important amounts (Delvaux et al. 2001).



104

105 **Figure 1. Geographical and geomorphological framework of the study area.** Lake's polygons from Esri,  
106 Garmin International, Inc.; topographic base from NASA's SRTM project (Far and Kobrick, 2000).

107 The mountain belts contain several regional fault zones, and others cross the mountain systems with a NW-SE axis  
108 (Trifonov et al. 1992). Paleozoic crystalline rocks form, for the most part, the mountain ridges which correspond  
109 to a neotectonic anticline and are separated by tectonic depressions, with lenticular or linear shapes. These  
110 intermountain depressions host the primary river valleys and are filled by Neogene and Quaternary deposits,  
111 principally sandstone, siltstone interbedded by gypsum, and conglomerates (Strom and Abdrakhmatov, 2017).  
112 Lithologies from Mesozoic and Paleogene are characteristic of the areas at the foot of mountain ranges. This main  
113 deeply incised river network, fed by glaciers, snowmelt water and rain, is linked by narrow deep gorges up to 1-2  
114 km deep (Strom and Abdrakhmatov, 2018) and is the origin of most of the rivers in Central Asia.

115 The retreat and shrinkage of glaciers in Central Asia regions induced by the global warming produce a seasonal  
116 variation in river discharge and consequently an increase of its induced hazards such as glacial lake outburst floods  
117 (GLOFs) resulting in countless losses of human life and destroyed infrastructure (Petrov et al. 2017; Wang et al.,  
118 2013). The high seismicity, frequent floods and a complex geological and topographic structure contribute to  
119 predispose the region to frequent landslides which can potentially obstruct the narrow valleys of the mountain  
120 ranges and in turn be the cause of chain risks (CAC DRMI, 2009; Havenit et al, 2017).




### 121 3 Materials and Methods

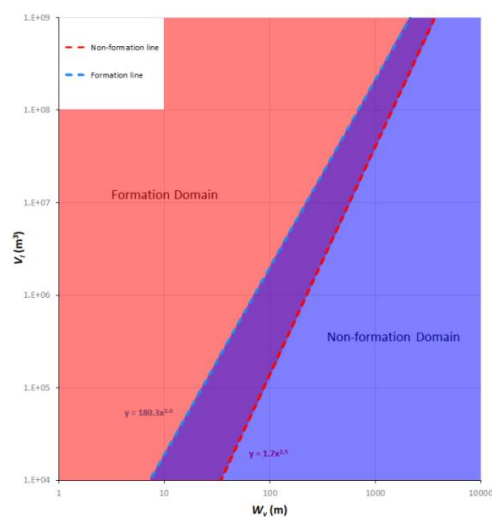
122 The Morphological Obstruction Index (MOI) (Tacconi Stefanelli et al., 2016) is a bivariate index able to evaluate  
123 the potential hazard posed by landslide dams that requires only simple morphometrical parameters which are easily  
124 extracted from common Digital Elevation Models. The MOI has been used in several studies, such as in Italy and  
125 Peru (Tacconi Stefanelli et al., 2016; 2018), to assess landslide damming susceptibility showing better results than  
126 others popular indexes (Swanson et al., 1986). It is a useful tool for identifying high-risk areas and for prioritizing  
127 mitigation efforts in landslide-prone regions.

128 The MOI is calculated by dividing the volume of the landslide,  $V_l$  ( $m^3$ ), by the width of the river valley,  $W_v$  (m),  
129 at the dam location.

$$130 \quad MOI = \log \left( \frac{V_l}{W_v} \right) \quad (1)$$

131 The MOI is based on the principle that the higher the ratio of the landslide volume to the river width, the greater  
132 the potential for dam formation. It is important to point out that river width,  $W_v$ , shall be defined as the width of  
133 the river valley which can potentially be obstructed creating a dammed lake and not of just the channel where the  
134 river flows.  is often misinterpreted, although in narrow mountain valleys these often coincide.

135 Landslide dams analyzed by the index can be grouped within three evolutionary classes: formed, not formed and  
136 of uncertain evolution. The limits of these domains are depicted by two lines, the lower red “Non-formation line”  
137 and the upper blue “Formation line” (Figure 2).



138

139 **Figure 2. Schematic plot of the non-Formation line and Formation line.**

140 The equation of the former is expressed as follows:

$$141 \quad V_l' = 1.7 \cdot W_v^{2.5} \quad (2)$$



142 Where  $V_1'$  is the “Non-formation volume” and is the minimum landslide volume able to potentially block a river  
143 with a given width  $W_v$ . Smaller volumes cannot completely dam the river. The latter expression draws the upper  
144 limit for not formed dams and is expressed as follows:

$$145 \quad V_1'' = 180.3 \cdot W_v^2 \quad (3)$$

146 Where  $V_1''$  is the “Formation volume”, is the minimum landslide volume able to dam the river valley, with a  
147 confidence of 99%, and the inferior boundary of the Formation domain (which includes only formed dams).

148 As originally proposed by Tacconi Stefanelli et al. (2020), these two equations, Eq.(2) and (3), can be used to  
149 apply a simple semi-automatic methodology in order to verify at basin scale the damming susceptibility from  
150 existing and neo-formed landslides. The following semi-automated procedure, inspired by the one of Tacconi  
151 Stefanelli et al. (2020) of which this represents an improvement, is applied on a national scale and can be  
152 reproduced entirely in a GIS (Geographic Information System) environment.

153 Within an even medium-long time interval the valley width in each river stretch does not change significantly and  
154 can be considered an immutable factor in the MOI equation (Eq.(1)). Starting from this assumption, along with  
155 Eq. (2) and Eq. (3), if the average river width  $W_v$  of each river stretch can be assessed, the two threshold landslide  
156 volumes  $V_1'$  (Non-formation volume) and  $V_1''$  (Formation volume) can be estimated for each river stretch.

157 Landslides that cause river obstruction are in many cases reactivations of ancient movements that are still in a  
158 condition of partial instability and that have not reached a potential equilibrium reaching the valley floor.  
159 Therefore, with a landslide inventory it is possible to assess, with some assumptions and simplifications, which  
160 among the mapped landslides are able to dam their river section. Each landslide that is not already laying in the  
161 valley floor with a volume bigger than  $V'$  and  $V''$  are identified as potentially prone to block the river in the future  
162 in that point. Then, a "Map of Damming Susceptibility" for reactivation of existing landslides can be generated.

163 The likelihood prediction for new landslides, with volume bigger than  $V_1'$  and  $V_1''$ , is a much more difficult task  
164 as the volume is a complex value to be estimated (Catani et al., 2016). The exceeding probability of landslide  
165 volume used by Tacconi Stefanelli et al. (2020) was reached thanks to the knowledge of the alpha exponent of the  
166 statistical frequency distribution of the landslide volumes in the whole study area. To achieve this, a database of  
167 landslides with a very high number of events (tens or even hundreds of thousands) should be available (Catani et  
168 al., 2016), which in our study area unfortunately is not. To have an assessment of the damming susceptibility for  
169 neo-formed landslides the two volume threshold values, evaluated for all the river networks, can be used as well.  
170 After estimating the river width of every river stretches, the  $V_1'$  and  $V_1''$  values of each of them can be computed  
171 through the corresponding two equations. In this way there will be two reference values to be able to assess whether  
172 the volume of a new landslide can potentially obstruct an affected river stretch.

173 The input data needed for the procedure are a Digital Elevation Model, a vector layer of the river network, and an  
174 updated landslide inventory. The data quality and resolution such as the landslides inventory completeness, the  
175 river network reliability and the DEM's pixel size heavily affect the quality of the result (Tacconi Stefanelli et al.,  
176 2020). Thus, it was decided to use the DEM with the higher resolution freely available from the NASA's SRTM  
177 project (Far and Kobrick, 2000) with a 1 arc-second, or about 30 meters of resolution. The river network came



178 from Coccia et al., (2023). The latter input data is a database of 8910 landslides, that is a compilation of several  
179 different inventories collected through decades of field surveys, studies and remote sensing analysis in the study  
180 area, shown in Figure 3.

181 Hereafter the detail of each inventory:

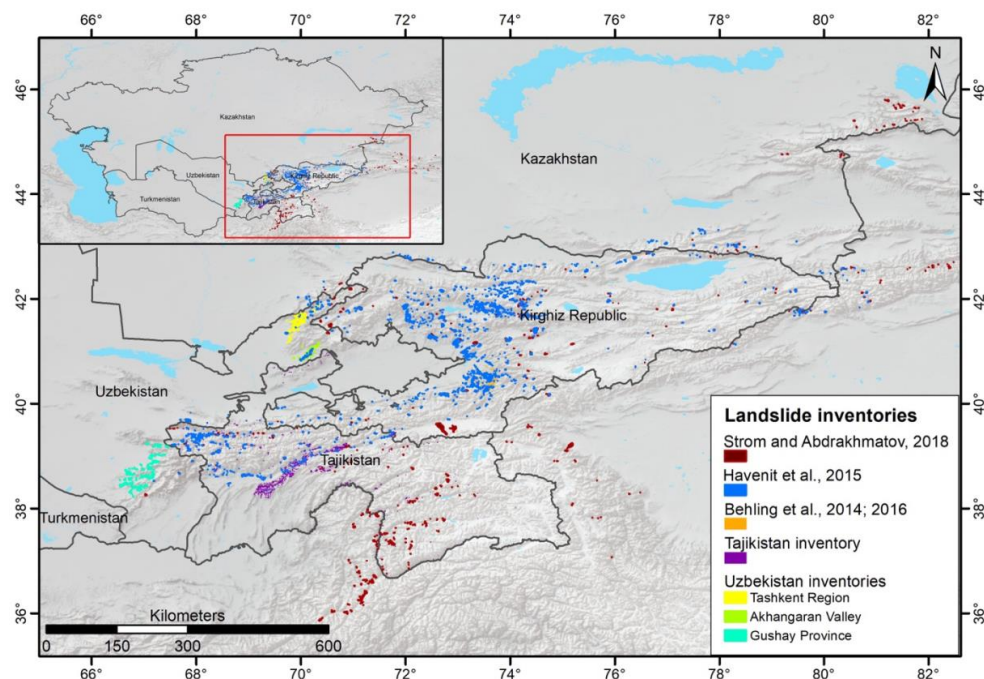
182 • The “Rockslides and Rock Avalanches of Central Asia” (Strom and Abdrakhmatov, 2018): an inventory  
183 including more than 1000 of very big ( $\geq 1 \text{ Mm}^3$ ) rockslides and rock avalanches, covering central Asian countries  
184 (excluding Turkmenistan and Altai) and also Chinese Tien Shan and Pamir, and Afghan Badakhshan. Collected  
185 in decades of field survey and analysis of aerial/satellite imaging, it includes also information on morphometric  
186 parameters (runout, area), dammed lakes, head-scarps, and quantitative characteristics (such as area, volume) for  
187 about 600 cases.

188 • The “Tien Shan landslide inventory” (Havenith et al., 2015a): is the biggest database in the study area.  
189 Assembled through field work, remote sensing and geophysical data interpretation, it includes the elements of the  
190 previous inventory alongside other smaller landslides in soft sediments (Havenith et al. 2006a; Schlögel et al.,  
191 2011) for a total of 3,462 landslides polygons, including information on landslide length and area.

192 • The “Multi-temporal landslide inventory for a study area in Southern Kyrgyz Republic derived from  
193 RapidEye satellite time series data (2009 – 2013)” (Behling et al., 2014; 2016; 2020), includes 1,582 landslide  
194 polygons mapped from multi-sensor optical satellite time series data (from 1986 to 2013) over an area of 2,500  
195  $\text{km}^2$  in the Fergana valley rim in southern Kyrgyz Republic, and include information on landslide activity (area  
196 and year of trigger).

197 • The “Tajikistan landslide database” produced by the Institute of Water Problems, Hydropower,  
198 Engineering and Ecology of Tajikistan (IWPHE), with 2,710 landslide polygons and 114 landslide-prone areas,  
199 including information on landslides length and area.

200 • The Institute of Seismology of the Academy of Science of Uzbekistan (ISASUZ) provided an inventory  
201 which covers the Tashkent province composed by a point inventory (Nyazov R.A. 2020) and a polygon inventory  
202 (345 landslide) digitized from the maps in Juliev et al., 2017.

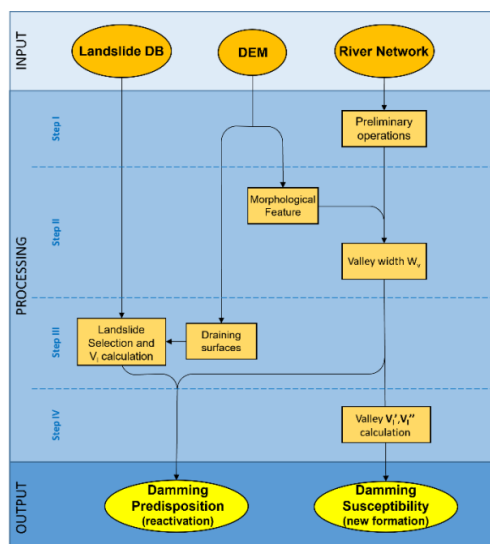


203

204 **Figure 3. Map of the landslide inventories in the study area.** Lake's polygons from Esri, Garmin  
205 International, Inc.; basemap from Esri, USGS, NOAA.

206 The methodology adopted to obtain the maps of damming susceptibility, derived from Tacconi Stefanelli et al.  
207 (2020), is summarized in the following main steps displayed in Figure 4. According to the literature (Swanson et  
208 al., 1986; Fan et al. 2014, 2020, 2021; Tacconi Stefanelli et al., 2015, 2018), river obstructions occur in most of  
209 the time within hilly or mountainous areas and specially along steep slopes. Therefore, considering the extension  
210 of the study area, in order to reduce the time of elaboration and improve the visualization of the results, in step I  
211 of Figure 4 a series of unnecessary data were removed from the calculations during some preliminary operations.  
212 For this reason, river that flow in flat areas (with less than 4° slopes) were not considered in the elaborations, since  
213 their damming probability is certainly very low, and the potential impounded lake should have a negligible volume.  
214 Additionally, to have maps easier to manage and display, the river network was split in 5 km long river stretches  
215 consecutive to each other.



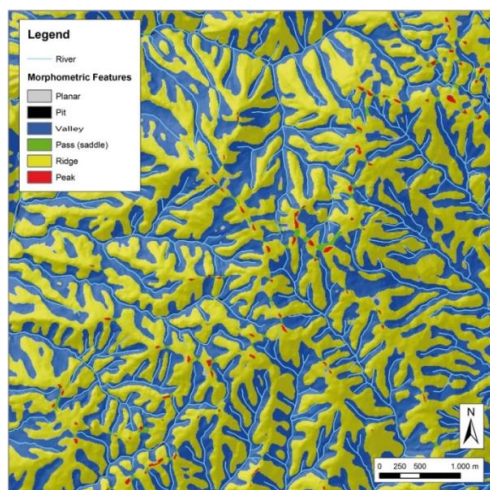


216

217 **Figure 4. Flow chart of the main steps of the mapping methodology.**

218 In applied geomorphology and natural science studies the analysis and characterization of the landscape has  
219 evolved during the last decades with the increasing accessibility of remote sensing data and the development of  
220 different algorithms able to automatically extract morphological features and landform information even at broad  
221 scales (Drăguț and Dornik 2016; Maxwell and Shobe 2022; Righini and Surian 2018; Wang et al. 2010).

222 As already mentioned, the clear definition of the width of a river can be subjective and its measurement difficult  
223 to repeat especially if performed by different operators. In step II of Figure 4, an objective automatic method to  
224 extract morphometrical parameters have been chosen also for this reason. Wood (2009) implemented the  
225 “*LandSerf*” software (already incorporated in SAGA GIS or QGIS software), designed to automatically classify  
226 landforms from DEMs. Similarly for pattern detection and texture analysis within image processing, the software  
227 extracts land-surface parameters (e.g., slope, aspect, and curvature) from DEMs through a multi-scale approach.  
228 During these processing, the algorithm performs a classification of the landscape, grouping the landforms with  
229 homogeneous morphometric characteristics (pits, channels, peaks, ridges, passes, and planes) as shown in Figure  
230 5. Thanks to this algorithm of morphological forms analysis proposed by Wood (2009), the polygons representing  
231 the morphological unit of the river valley can be automatically defined objectively even in a large area and  
232 extracted.



233

234 **Figure 5. Classification of the landscape into morphological classes according to Wood (2009) (modified**  
235 **from Tacconi Stefanelli et al., 2020).**

236 The effectiveness of distinguishing different morphological landforms of this automatic tool is greater in  
237 mountainous regions characterized by significant differences in elevation, compared to flat areas where  
238 distinctions between landforms are less evident. The accuracy of the output is directly correlated with the resolution  
239 of the DEM, which should ideally be about a few meters. Coarser resolutions result in landslide volumes with a  
240 corresponding level of uncertainty.

241 The following phase is to provide to each river stretch a value of a valley width,  $W_v$ . A series of 1 km long lines  
242 (hereafter “transects”) are generated, perpendicular to the stretches of the river network, outdistanced by 500  
243 meters apart from each other. The created river valley polygons are used to “cut” the transects and then to measure  
244 the distance between the two river valley borders through the length of the cut transects.

245 Next, the valley widths ( $W_v$ ) for each segment of the river are determined by assigning them an average value  
246 based on  $N$  perpendicular transects, excluding the extreme values (maximum and minimum, respectively  $W_{max}$   
247 and  $W_{min}$ ), as in the following equation:

$$248 \quad W_v = \left( \sum_{i=1}^n W_i - W_{min} - W_{max} \right) \frac{1}{n-2} \quad (4)$$

249 By utilizing an updated database of landslide polygons, in the step III of Figure 4 it is possible to determine if a  
250 reactivated landslide is big enough to cause a complete river blockage thanks to the comparison with the boundary  
251 volumes of  $V_i'$  (below which a landslide cannot completely block the river) and  $V_i''$  (above which the river valley  
252 is dammed for sure). A reactivated landslide should follow a downhill path akin to the flow of surface water.  
253 Within each slope, the drainage directions can be easily determined along the river network using a GIS software.  
254 Each mass movement can then be linked to the corresponding river stretch it would reach if reactivated based on  
255 their corresponding draining surfaces.



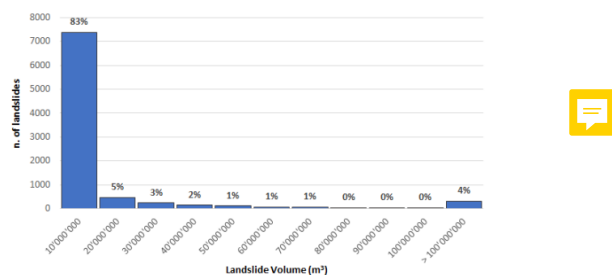
256 Since the information provided by the available inventories in the study area are not homogeneous and comparable,  
 257 for the computation of the landslide volume were chose to use the areas of the landslide polygons, since it is the  
 258 most common data. An experimental statistical relationship between areas and volumes was applied:

$$259 \quad V_l = \varepsilon \cdot A_l^\alpha \quad (5)$$

260 where  $V_l$  and  $A_l$  are respectively the volume and the area of a landslide,  $\varepsilon$  and  $\alpha$  are respectively the constant and  
 261 the exponent of the power law describing the landslides volumes frequency distribution. Various experimental  
 262 relations of  $\varepsilon$  and  $\alpha$  have been employed for landslide volume calculations by researchers located in different  
 263 countries. After an evaluation of these relations in the study area, the parameter proposed by Guzzetti et al. (2009)  
 264 have been selected because of the number of the studied cases (667) and the magnitude range of the landslides  
 265 area investigated (from  $10^1$  to  $10^9$  m<sup>2</sup>). The landslide volume computed using this procedure is based on some  
 266 approximations, since they use geometric simplifications, but it does still reflect the magnitude of the process. The  
 267 result of the computation in Figure 6 shows an almost bimodal distribution, in which most landslides (83%) have  
 268 moderate volumes, lower than 10 million m<sup>3</sup> (with 63% lower than 1 million m<sup>3</sup>), but 4% have value higher than  
 269 100 million m<sup>3</sup>.

270 Then, Table 1 is used to assign to each landslide of the inventory a classification based on the comparison with the  
 271 boundary volumes  $V_l'$  and  $V_l''$ , with value of 2 if the calculated landslide volume,  $V_l$ , is bigger than  $V_l'$  (or  $V_l''$ ),  
 272 of 0 if it is smaller. For more caution, the  $V_l$  values is increased by an arbitrary value of 20% ( $V_l \cdot 1.2$ ) to avoid  
 273 any potential underestimation during volume estimation and even the possible increase of landslide size with the  
 274 reactivation due to the mechanism of material entrainment (Hungur & Evans, 2004). For each landslide, if the  
 275 computed boundary volume  $V_l'$  (or  $V_l''$ ) is bigger than the estimated landslide volume  $V_l$ , but smaller than  $V_l \cdot$   
 276 1.2, then a classification value of 1 is attributed.

277 The damming susceptibility of each mapped landslide is assigned by integrating the two comparative classification  
 278 values from the intensity matrix illustrated in Figure 7. The matrix establishes five qualitative classes on a scale  
 279 of severity for damming susceptibility, ranging from Very Low (dark green) to Low (light green), Moderate  
 280 (yellow), High (orange), and Very High (red). The combination of a high  $V_l''$  value (1 or 2) and a lower  $V_l'$  value  
 281 (0 or 1) symbolized by gray squares is not possible according to their respective formulations.



282

283 **Figure 6. Landslide volumes frequency distribution in the central Asia regions.**

284 **Table 1. Comparison table between landslide calculated volumes,  $V_l$ , with the boundary volume of Non-**  
 285 **formation and Formation,  $V_l'$  and  $V_l''$  (after Tacconi Stefanelli et al., 2020).**



	$V_1 > V_1' (V_1'')$	$V_1 < V_1' (V_1'') < V_1 * 1.2$	$V_1 < V_1' (V_1'')$
Classification Value	2	1	0

286

$V_1' \backslash V_1''$	0	1	2
0	Very Low		
1	Low	Moderate	
2	Moderate	High	Very High

287

288 **Figure 7. Predisposition matrix used for the assignment of the damming predisposition intensity to the**  
 289 **mapped landslides (after Tacconi Stefanelli et al., 2020).**

290 Even if the proposed method is objective, it is certainly not free from uncertainties and errors. The 20% increase  
 291 applied to mapped landslide volumes to reduce underestimation errors can in turn produce false positives for  
 292 overestimation errors. While a false positive is preferable to a false negative (according to a principle of prudence),  
 293 too many high-risk false positive cases "spread" an unreal risk throughout the area instead of concentrating it in  
 294 sites of real risk. Therefore, it can be assumed that the landslide bodies which have previously reached the valley  
 295 floor have already generated most of their effect on the river network (Strom, 2010) or have had no effect, spending  
 296 their potential risk component. These landslides, also with a volume higher than  $V_1'$  and  $V_1''$  and therefore classified  
 297 with Very High dam predisposition, even if reactivated probably will not produce any further effect in the future.  
 298 For these reasons, it was decided to downgrade the classification of those landslides that intersect the river network  
 299 by reducing its position of the classification of damming predisposition by one class.

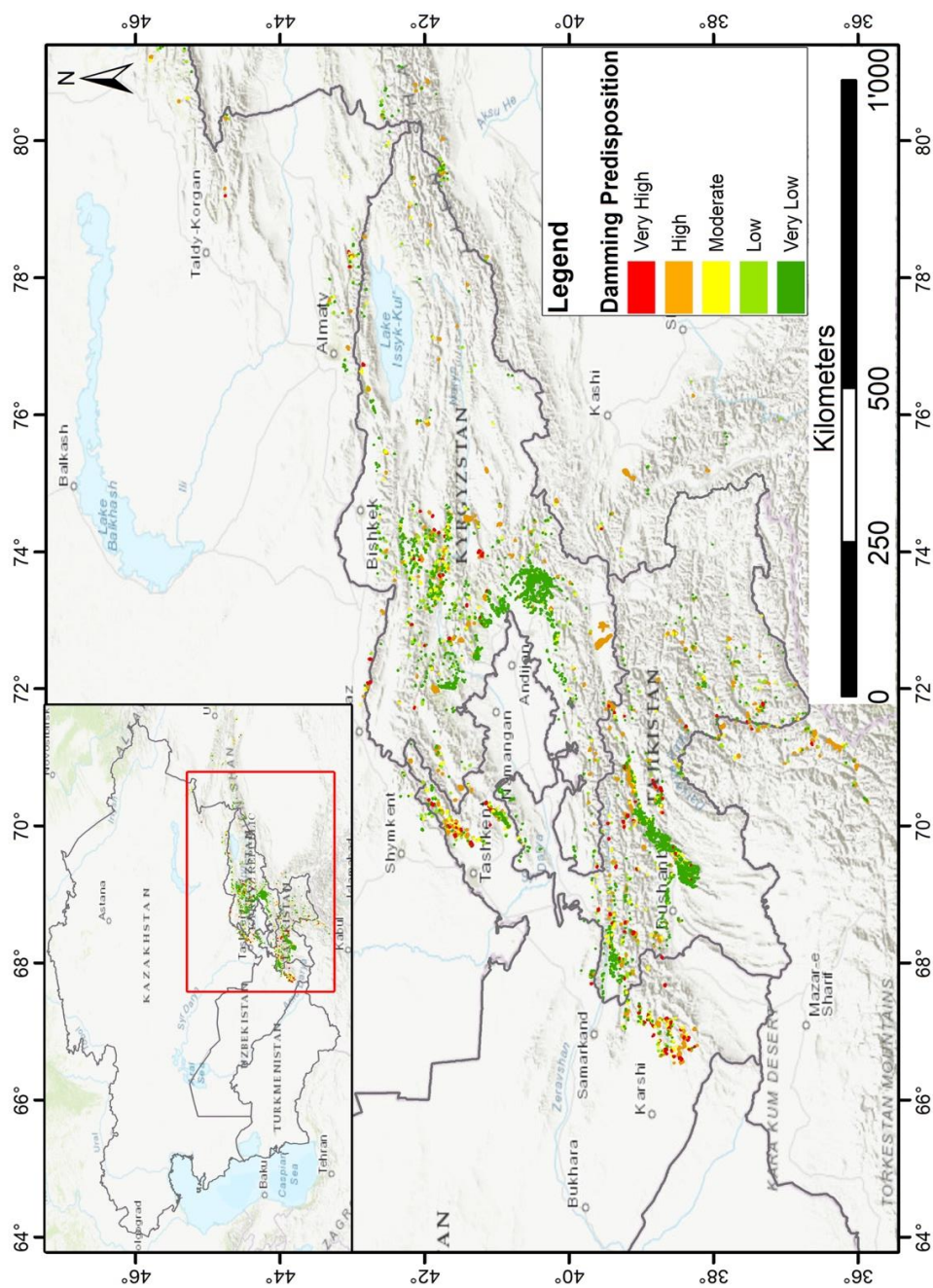
300 Using the  $W_v$  value for each river stretches estimated during the step III of Figure 4, in the last step (IV) the two  
 301 boundary landslide volumes, namely "Non-formation volume" and "Formation volume" ( $V_1'$  and  $V_1''$ ), can be  
 302 estimated by applying the equations of the "Non-formation" (Eq. (2)) and "Formation" lines (Eq. (3)). These two  
 303 values can be used both to classify the damming susceptibility of the river network (for new landslides) and of the  
 304 landslides inventory (for their reactivation). For the first case, the computed volume values  $V_1'$  and  $V_1''$  embody  
 305 the required volumes of a new landslide to have a potential or certain (with 99% of confidence) obstruction for  
 306 each river stretches.



307 **4 Results**

308 The mapping methodology was applied to all the studied territories of the Central Asia region in order to analyze  
309 and evaluate the results. Two smaller basins, the upper Pskem river and the Fergana valley, were selected to verify  
310 the reliability at a catchment scale of the results obtained from a methodology applied on a national scale. The  
311 assessment of damming predisposition on the available landslide inventory on the Central Asia regions is shown  
312 in the map of Figure 8, while a closer detail is reported in Figure 10 showing the Kyrgyz Republic territory. The  
313 number of landslides (644 cases) classified with Very High damming predisposition from the whole inventory  
314 before the class reduction due to the river intersection was unjustifiably and unreasonably large posing excessive  
315 concern and risk perception. After the change, this number decreased by 75% up to 166 cases, a high number but  
316 more reasonable concerning such a large area. In the class distribution of the damming predisposition shown in  
317 Figure 9 the most frequent class is the Very Low, with 81% of the whole database, followed by the Low and High  
318 classes both with 6% and the remaining percentage divided among Moderate (5%) and Very High (2%).

319 This distribution is quite coherent with the landslide volumes frequency distribution since it is reasonable to  
320 associate landslides with very low volume (83%, shown in Figure 6) with those classified with very low  
321 susceptibility (81%, Figure 9). The landslides classified with the higher values of susceptibility (Moderate, High,  
322 and Very High with a total of 13%) instead do not only include landslides with higher volumes (more than 100  
323 million m<sup>3</sup> representing 4% of the total), meaning that also even smaller landslides can potentially block narrow  
324 river stretches in these regions.



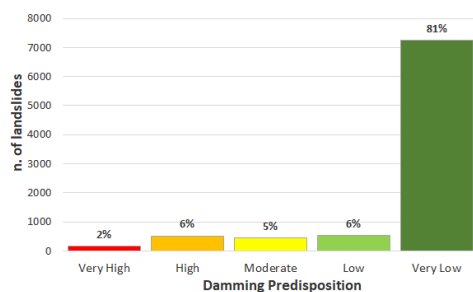
325

326 **Figure 8. Map of Central Asia Landslide Damming Susceptibility.** Basemap source: Esri, HERE, Garmin  
327 Intermap, increment P Corp, GEBCO, USGS, FAO, NPS, NRCAN, GeoBase, IGN, Kadaster NL, Ordnance



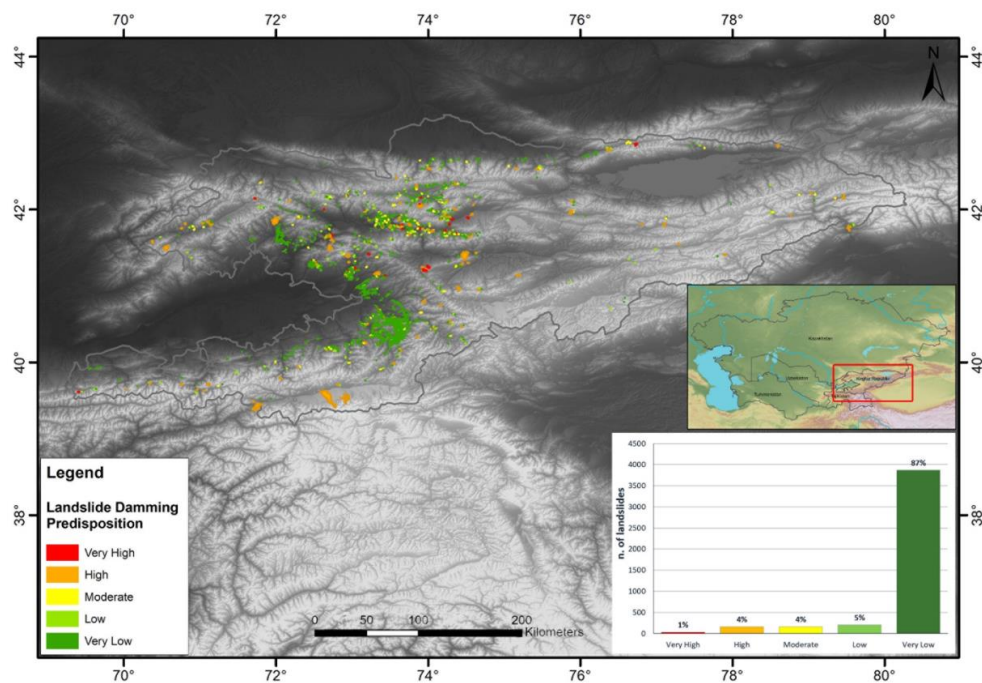
328 Survey, Esri Japan, METI, Esri China (Honk Kong), © OpenStreetMap contributors, and the GIS User  
329 Community.

330



331

332 **Figure 9. Classes distribution of the damming predisposition for landslides reactivation.**



333

334 **Figure 10. Map of Damming Predisposition by landslides reactivation in Kyrgyz Republic territory.**

335 Topographic base from NASA's SRTM project (Far and Kobrick, 2000).

336 Concerning the damming susceptibility caused by new landslides along all the river network in the study area, two  
337 different maps of the river networks have been produced using the Non-formation and Formation volumes values.  
338 Although counterintuitive at first glance, these maps provide complementary information. The former provides  
339 the volumes of landslides that surely create an obstruction, while the latter the volumes below which it definitely

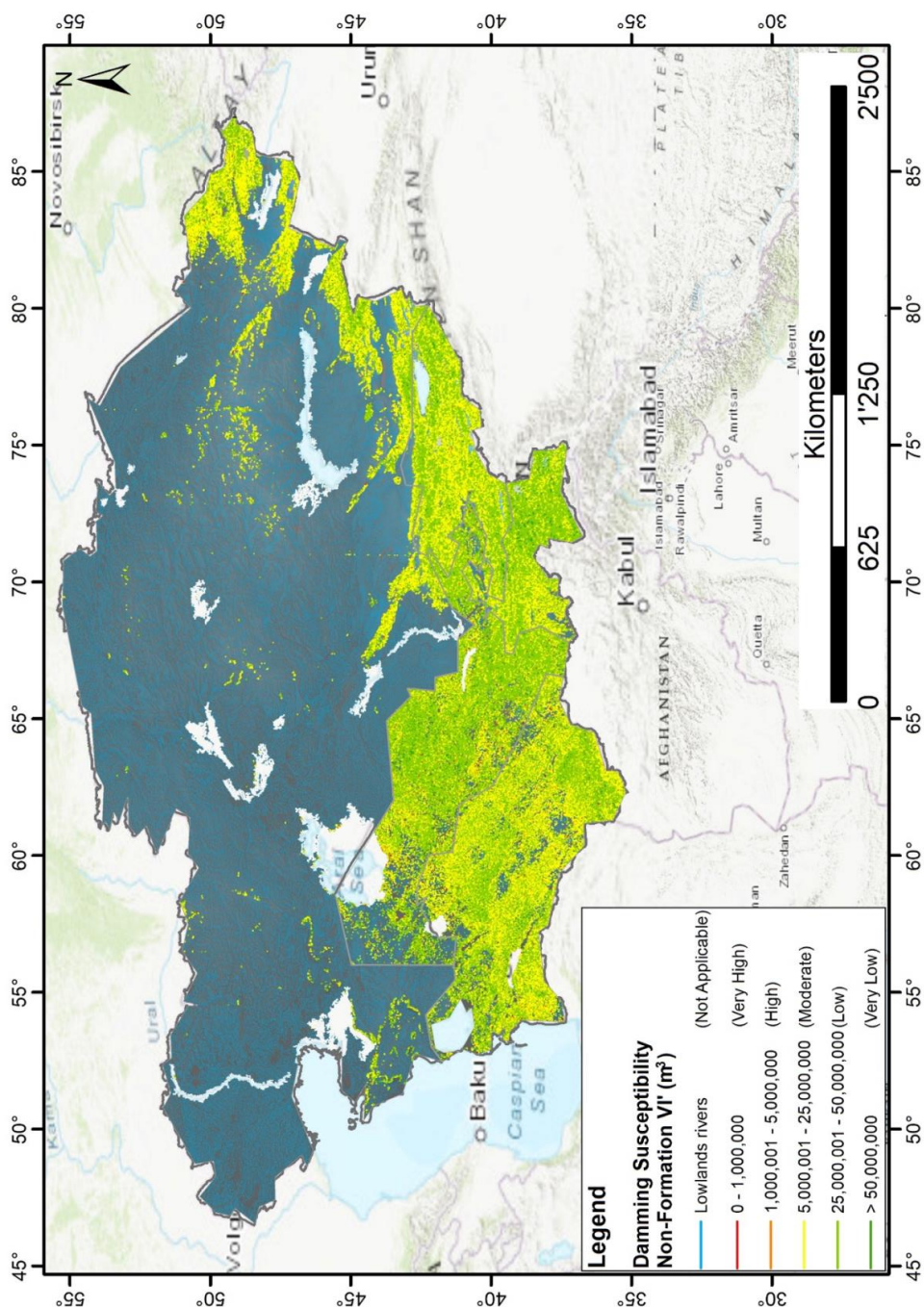


340 does not form. According to the preliminary steps of the described methodology, in the river stretches running in  
341 flat areas (slope degree less than  $4^\circ$  representing the 88.4% of the entire river network) the analysis has been not  
342 applied, due to the extreme unlikelihood that a complete obstruction will occur in such areas. The magnitude of  
343 the damming susceptibility of the river networks has been classified in five classes and shown in Figure 11 and  
344 Figure 14. The five volumes intervals describing damming susceptibility were decided according to general value  
345 distribution of landslides volumes and an expert judgement. Since small landslides are more frequent than large  
346 ones, as reported in Figure 6, the lower is the landslide volume required to realize an obstruction, the higher is the  
347 magnitude. In the map of damming susceptibility related to the “Non formation”, reported in Figure 11, the central  
348 classes, Moderate and Low are the most frequent with 4.4% and 5.8% respectively, as reported in Figure 12. This  
349 means that in most of the river stretches in the study area the minimum landslide volume able to potentially dam  
350 the riverbed is between the limit values of the two classes, from 2,5 to 25 million  $m^3$ . The following most frequent  
351 class is the Very Low with 0.8% and only a very small portion of the river stretches are classified as High and  
352 Very High with just 0.4% and 0.2% with a required landslide volume less than 2.5 million  $m^3$ . An example of  
353 close-up on the Tajikistan territory is reported in Figure 13.

354 Regarding the map of damming susceptibility related to Formation values, the map in Figure 14 shows slightly  
355 different results. The most frequent classes are the two lower ones, Low and Very Low with 4.4% and 6%  
356 respectively, as described in Figure 15. Only just the 0.3% and 0.4% fall in the classes Very High and High  
357 damming susceptibility. A close-up on the Kyrgyz Republic is reported in Figure 16.

358 The results of the classification for the river networks of each state are shown in Figure 17 to Figure 21. The  
359 landslides of Tajikistan, Kyrgyz Republic, Uzbekistan and Kazakhstan regions have been classified according to  
360 damming predisposition (Figure 17-a., Figure 18-a., Figure 19-a. and Figure 20-a.). In the Turkmenistan territory,  
361 it was not possible to assess any damming predisposition by landslides reactivation since the absence of any  
362 available landslide inventory. The results of Uzbekistan and Kazakhstan regions (Figure 19-a. and Figure 20-a.)  
363 are a bit different from Kyrgyz Republic and Tajikistan regions due to the different availability of landslide  
364 inventories and a different reliefs orographic structure and valleys morphology of the former national territories.  
365 As already mentioned, for a clearer comprehension of the damming susceptibility classification of the river  
366 network at the national level, the river stretches flowing in lowlands have not been considered in the analysis.  
367 Concerning the Damming Susceptibility of Non-Formation (Figure 17-b., Figure 18-b., Figure 19-b., Figure 20-b.  
368 and Figure 21-a.), the most frequent are Low and Moderate classes, followed by Very Low class. Fortunately, only  
369 very few river stretches have been classified as Very High and High. For the Damming Susceptibility of Formation  
370 (Figure 17-c., Figure 18-c., Figure 19-c., Figure 20-c. and Figure 21-b.) most of the rivers fall into Very Low and  
371 Low classes, followed by Moderate class. Also in this case, only very few river stretches have been classified as  
372 Very High and High. The results of the Tajikistan territory are quite similar to the Kyrgyz Republic and Uzbekistan  
373 with which it shares a similar orographic distribution and morphology of the territory. Turkmenistan and  
374 Kazakhstan show a slightly different distribution with higher percentage on Moderate class in the Damming  
375 Susceptibility of Non-Formation and Low class in the damming susceptibility of Formation.



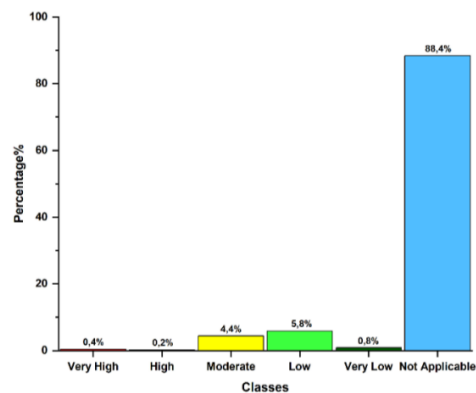


376

377 **Figure 11. Damming susceptibility map of non-formation of river stretches by new landslides in the**  
378 **region.** River network database from Coccia et al., (in prep.). Basemap source: Esri, HERE, Garmin Intermap,

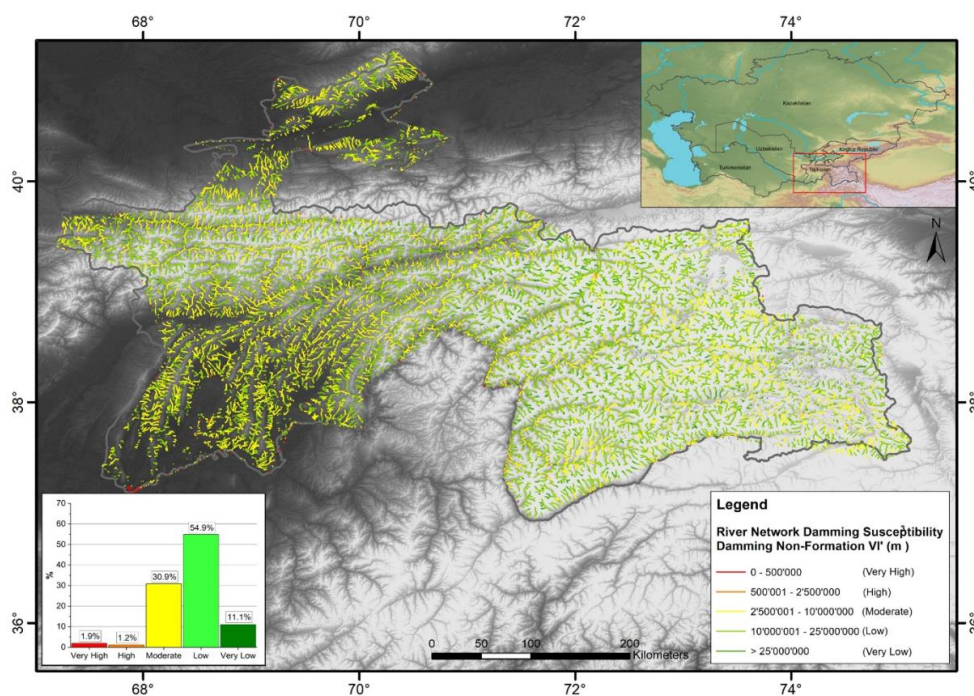


379 increment P Corp, GEBCO, USGS, FAO, NPS, NRCAN, GeoBase, IGN, Kadaster NL, Ordnance Survey, Esri  
380 Japan, METI, Esri China (Honk Kong), © OpenStreetMap contributors, and the GIS User Community.



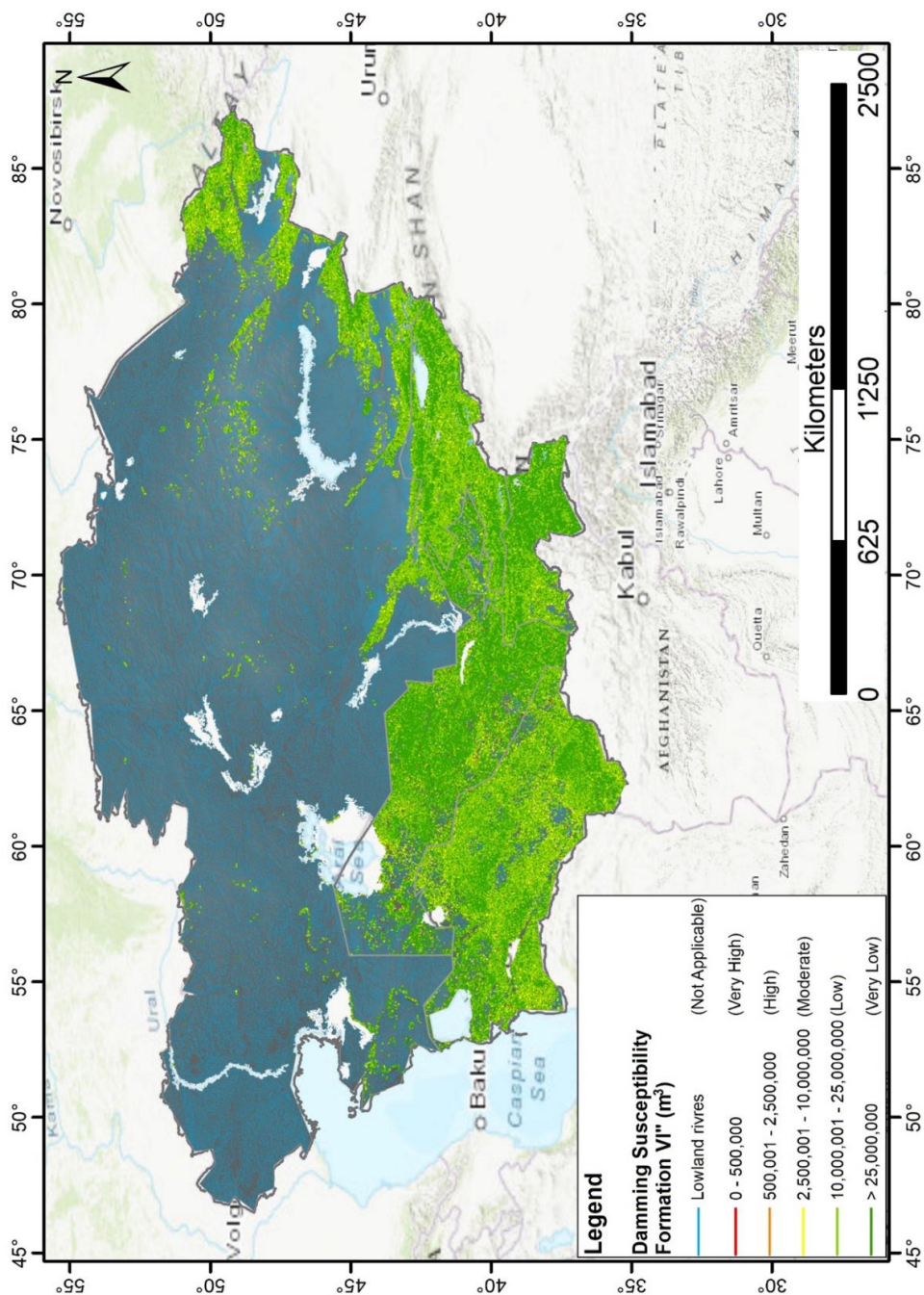
381

382 **Figure 12. Distribution of the damming susceptibility in the study area by new landslides related to Non**  
383 **formation boundary values.**



384

385 **Figure 13. Damming Susceptibility Map of non-formation of river stretches by new landslides in**  
386 **Tajikistan.** River network database from Coccia et al., (in prep.). Topographic base from NASA's SRTM  
387 project (Far and Kobrick, 2000).



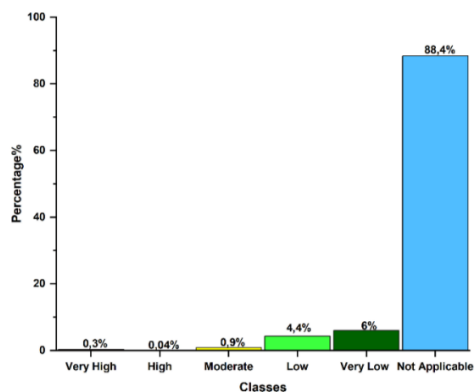
388

389 **Figure 14. Damming Susceptibility Map of Formation of river stretches by new landslides in the region.**

390 River network database from Coccia et al., (in prep.). Basemap source: Esri, HERE, Garmin Intermap, increment

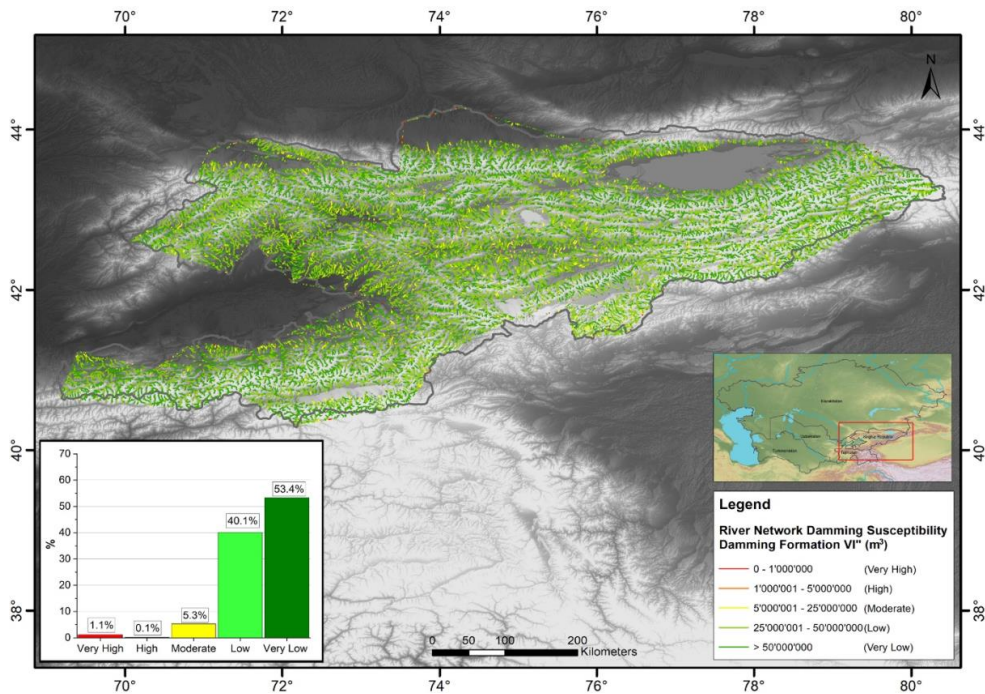


391 P Corp, GEBCO, USGS, FAO, NPS, NRCAN, GeoBase, IGN, Kadaster NL, Ordnance Survey, Esri Japan,  
 392 METI, Esri China (Honk Kong), © OpenStreetMap contributors, and the GIS User Community.



393

394 **Figure 15. Distribution of the Damming Susceptibility in the study area by new landslides related to**  
 395 **Formation boundary values.**

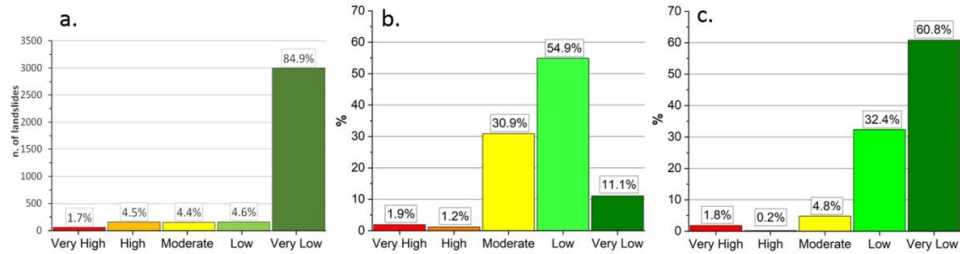


396

397 **Figure 16. Damming Susceptibility Map of formation of river stretches by new landslides in the Kyrgyz**  
 398 **Republic territory.** River network database from Coccia et al., (in prep.). Topographic base from NASA's  
 399 SRTM project (Far and Kobrick, 2000).



400



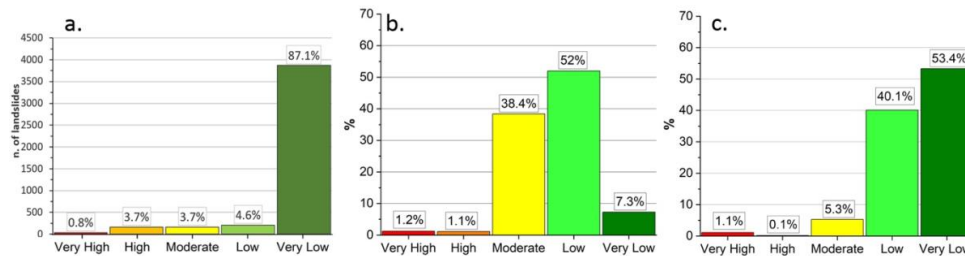
401

**Figure 17. Classes distribution in Tajikistan of the Damming Predisposition for landslides reactivation**

402

**(a.), Damming Susceptibility of Non-Formation (b.) and of Formation (c.) for new landslides.**

403



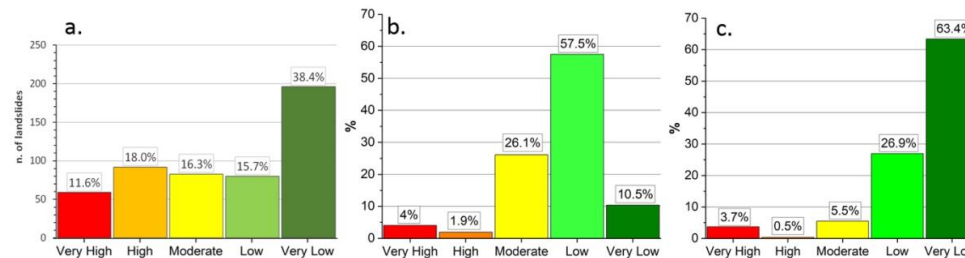
404

**Figure 18. Classes distribution in the Kyrgyz Republic of the Damming Predisposition for landslides**

405

**reactivation (a.), Damming Susceptibility of Non-Formation (b.) and of Formation (c.) for new landslides.**

406



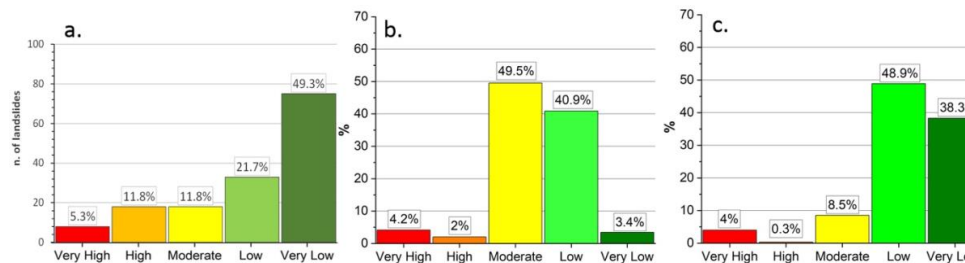
407

**Figure 19. Classes distribution in Uzbekistan of the Damming Predisposition for landslides reactivation**

408

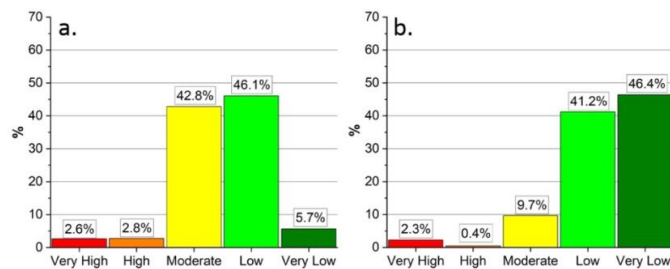
**(a.), Damming Susceptibility of Non-Formation (b.) and of Formation (c.) for new landslides.**

409





410 **Figure 20. Classes distribution in Kazakhstan of the Damming Predisposition for landslides reactivation**  
 411 **(a.), Damming Susceptibility of Non-Formation (b.) and of Formation (c.) for new landslides.**



412

413 **Figure 21. Classes distribution in Turkmenistan of the Damming Susceptibility of Non-Formation (a.) and**  
 414 **of Formation (b.) for new landslides.**

#### 415 **4.1 Upper Pskem river valley (Uzbekistan)**

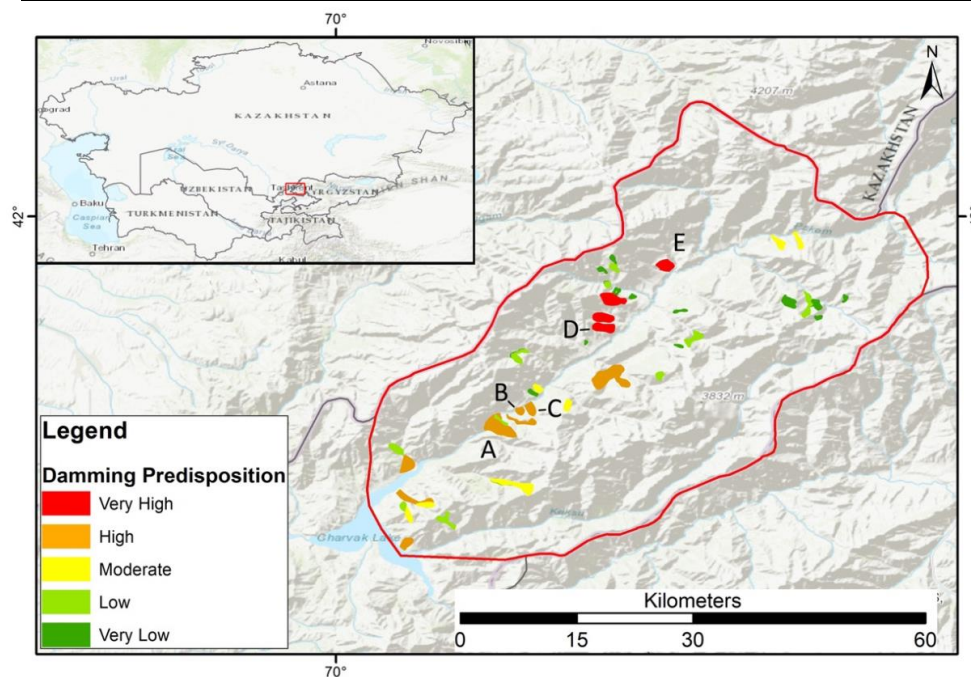
416 The Pskem river, locate in the Tashkent region of Uzbekistan, is a right-hand tributary of the Chirchik River that  
 417 is the feeder of the Syr Darya river basin (in the Western Tien-Shan). The river originates from the confluence of  
 418 the Maidantal and Oygaing rivers and is one of the main tributaries of the Charvak Lake (Semakova et al., 2016).  
 419 This artificial lake is central for the local economy for its functions as reserve for fishing and water, as well as a  
 420 source of hydroelectric energy and because of that various villages arise around it and downstream. The formation  
 421 of a natural obstruction and an upstream impoundment in the Pskem basin could be a serious threat due to the  
 422 possible instability of the earth dam and for the possible catastrophic cascade effects that its collapse could have  
 423 downstream on the artificial basins and their 168 meters high earthfill dam.

424 With a careful observation of the map of Damming Predisposition by landslides reactivation in the lower Pskem  
 425 basin in an area of 443 km<sup>2</sup> (Figure 22), some of the 53 mapped landslides should be subjected to further study.  
 426 Among all, most landslides were classified with a Very Low and Low predisposition value, respectively 21 and  
 427 11 cases (39.6% and 20.8%), and only 4 landslides with a Very High value (7.5%), 10 with High (18.9%) and 7  
 428 with Moderate (13.2%). Landslides named A, B, C, D and E in Figure 22, if reactivated will potentially cause an  
 429 obstruction of the main river section of the Pskem, being classified the first three and the latest two respectively  
 430 with High and Very High damming predisposition. As shown in Table 2, the volumes of all these landslides are  
 431 way bigger than the boundary volume of Non-Formation and Formation from Figure 23 and Figure 24. It is  
 432 important to notice that the landslides A, B and C are laid down in the valley floor, meaning that in the past they  
 433 had probably already dammed the river in that point, and the classification of their damming predisposition have  
 434 been reduced by one, from Very High to High. Due to the considerable volumes of the landslides in the basin and  
 435 the presence of landslides that have probably already blocked the river in the past, this relatively small area is  
 436 certainly worthy of attention.

437 **Table 2. Landslides volumes and damming parameters  $W_v$ ,  $V_1'$ ,  $V_1''$  of the landslides in Figure 20**  
 438 **computed using the described method.**



Landslide	$V_l$ - Landslide volume (m <sup>3</sup> )	$W_r$ - River Width (m)	$V_l'$ - Volume of Non-formation (m <sup>3</sup> )	$V_l''$ - Volume of Formation (m <sup>3</sup> )
A	200.000.000	300	2.600.000	16.200.000
B	12.000.000	235	1.500.000	10.000.000
C	34.000.000	318	3.000.000	18.200.000
D	73.000.000	513	10.100.000	47.400.000
E	61.000.000	575	13.500.000	60.000.000



439

440 **Figure 22. Map of Damming Predisposition by landslides reactivation in the lower Pskem basin.** Basemap  
 441 source: Esri, HERE, Garmin Intermap, increment P Corp, GEBCO, USGS, FAO, NPS, NRCAN, GeoBase, IGN,  
 442 Kadaster NL, Ordnance Survey, Esri Japan, METI, Esri China (Honk Kong), © OpenStreetMap contributors,  
 443 and the GIS User Community.

444 The obstruction of the Pskem river by one of these landslides would cause an upstream impoundment with a  
 445 surface from 2 to 10 km<sup>2</sup> or more, depending on the dam position and height. The dam collapse could release a  
 446 catastrophic flooding wave with destructive effects in the downstream areas. In the worst scenario, even the  
 447 earthfill dam located few kilometers downstream could be seriously damaged with unpredictable effects. Since the  
 448 reliability of this mapping method is strictly correlated to the quality of the input data, when the used DEM has a  
 449 coarse resolution, in similar cases of possible risk to people's life it is always advisable to do a second "manual



450 check" even using some free satellite imaging services like Google Earth. In fact, when the DEM resolution is too  
 451 rough, the GIS tool used in this methodology to evaluate the extension of the riverbed morphologic unit can  
 452 produce inconsistent and incorrect results, causing improper damming susceptibility evaluations. The results of  
 453 the measurements on Google Earth orthophotos in Table 3 show that the difference between the river width values  
 454 calculated with the mapping method ( $W_v$ ) and those measured on Google Earth ( $W_{vGE}$ ) can in some cases be  
 455 substantial modifying the calculated boundary volumes  $V'$  and  $V''$ , although in this case they do not modify  
 456 drastically the final classification of the five landslides.

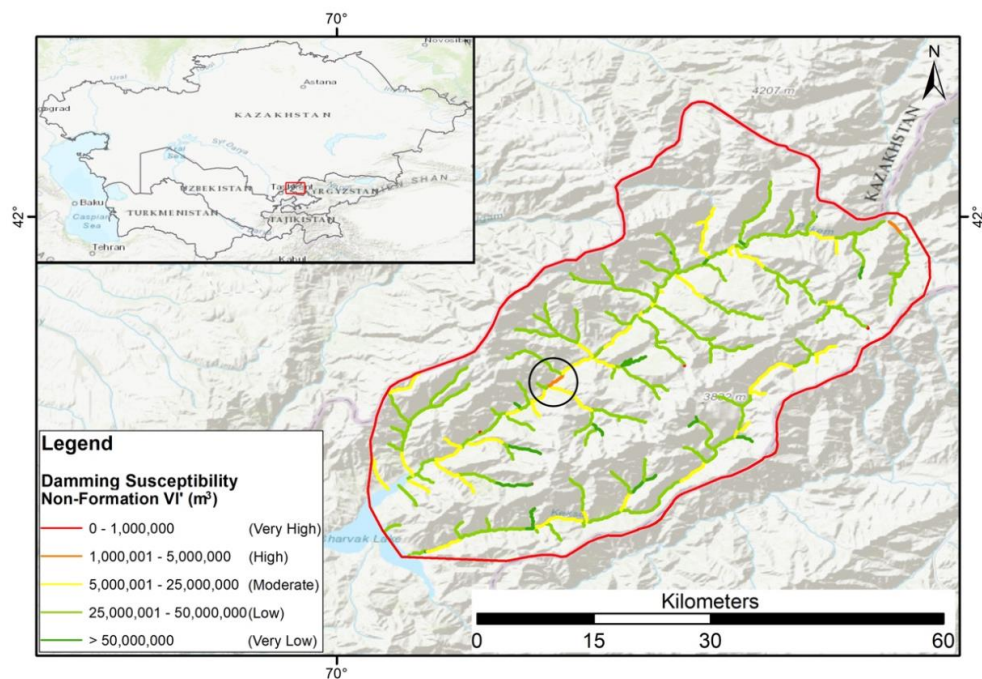
457 The river network of the upper Pskem valley have been also classified producing the maps of Damming  
 458 Susceptibility of Non-formation and Formation (Figure 23 and Figure 24 respectively). Concerning the Damming  
 459 Susceptibility Map of Non-formation (Figure 23), the most frequent are Low and Moderate classes with 65.1%  
 460 and 22.6% respectively, followed by Very Low class with 11.1%. Only just 1.3% have been classified as High and  
 461 0.0% as Very High. For the Damming Susceptibility Map of Formation (Figure 24) most of the rivers fall into  
 462 Very Low and Low classes with 69.8% and 27.7%, followed by Moderate class with 2.1%. Only 0.4% have been  
 463 classified as High and 0.0% as Very High.

464 **Table 3. Damming parameters  $W_{vGE}$ ,  $V'_{vGE}$ ,  $V''_{vGE}$  of the landslides in Figure 22 computed with Google**  
 465 **Earth observation.**

Landslide	$W_{vGE}$ – River Width (m)	$V'_{vGE}$ - Volume of non-formation (m <sup>3</sup> )	$V''_{vGE}$ - Volume of Formation (m <sup>3</sup> )
A	415	6.000.000	31.000.000
B	310	2.800.000	17.300.000
C	260	1.800.000	12.100.000
D	530	11.000.000	50.000.000
E	450	7.300.000	36.500.000

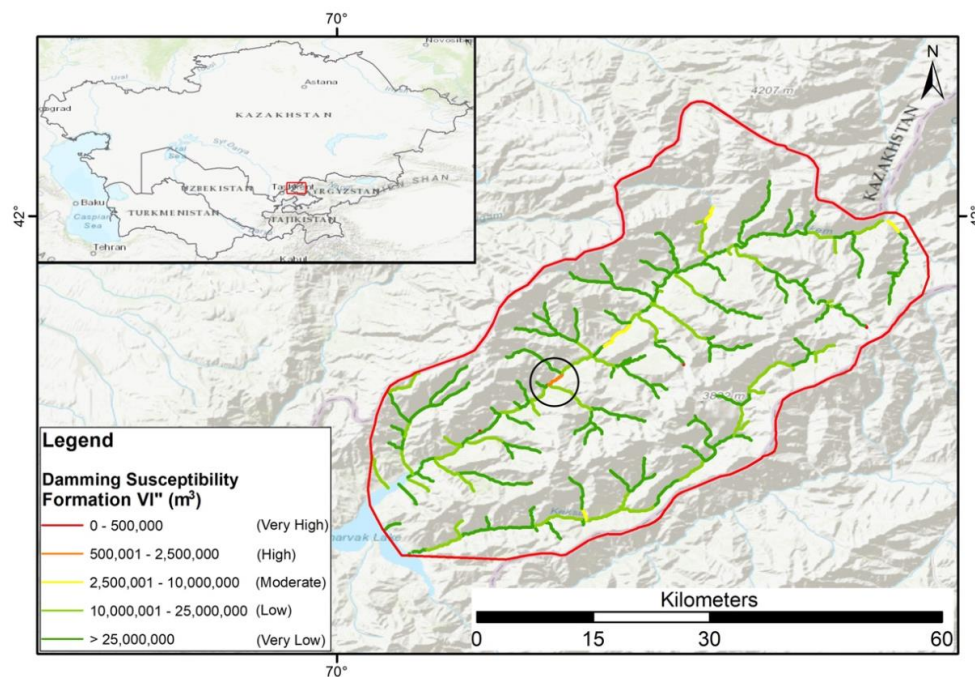
466  
 467 The general damming susceptibility of the valley is low but a singular river stretch, marked by a black circle in  
 468 Figure 23 and Figure 24, classified with High susceptibility in both maps should be carefully evaluated. This river  
 469 part is clearly noticeable in the middle of the area along the main river path, a bit upstream from the landslides  
 470 named B and C. The high classification values mean that geographically in that point the valley width undergoes  
 471 a shrinkage and for this reason even a relatively small landslide generated from the surrounding slopes can create  
 472 an obstruction, therefore it would be worthy of a more detailed investigation.





473

474 **Figure 23. Damming Susceptibility Map of Non-formation of river stretches by new landslides in the lower**  
475 **Pskem basin. The black circle highlights a river stretch with unusually high values.** River network database  
476 from Coccia et al., (in prep.). Basemap source: Esri, HERE, Garmin Intermap, increment P Corp, GEBCO,  
477 USGS, FAO, NPS, NRCAN, GeoBase, IGN, Kadaster NL, Ordnance Survey, Esri Japan, METI, Esri China  
478 (Honk Kong), © OpenStreetMap contributors, and the GIS User Community.



479

480 **Figure 24. Damming Susceptibility Map of Formation of river stretches by new landslides in the lower**  
481 **Pskem basin. The black circle highlights a river stretch with unusually high values.** River network database  
482 from Coccia et al., (in prep.). Basemap source: Esri, HERE, Garmin Intermap, increment P Corp, GEBCO,  
483 USGS, FAO, NPS, NRCAN, GeoBase, IGN, Kadaster NL, Ordnance Survey, Esri Japan, METI, Esri China  
484 (Honk Kong), © OpenStreetMap contributors, and the GIS User Community.

## 485 4.2 The Fergana valley mountainous rim (Tajikistan-Kyrgyz Republic- 486 Uzbekistan)

487 The Fergana valley is one of the largest intermountain depressions in Central Asia located between Uzbekistan,  
488 Kyrgyz Republic, and Tajikistan. It hosts two main rivers, the Naryn and the Kara Darya, which join together to  
489 form the Syr Darya. In this populated area landslide activity is recurrent, causing every year damage to  
490 infrastructure and loss of human life, and triggered by complex interactions between multiple factors such as  
491 tectonic, geological, morphological and meteorological (Danneels et al., 2008; Schläegel et al., 2011; Pironon et  
492 al., 2020). The mapping methodology have been applied also to the Fergana valley and a total of 3370 landslides,  
493 coming from various data sources, have been classified as shown in Figure 25. Comparably to the classification  
494 result of the entire inventory (Figure 8) most of the cases (94%) have a Very Low damming predisposition,  
495 followed by Low and Moderate (with 2.5% and 1.8% respectively) as reported in Table 4. Just very few landslides  
496 fall into High and Very High classes (with 1.4% and 0.3% respectively). For the classification of the river network  
497 of the Fergana valley, the maps of Damming Susceptibility of Non-formation and Formation have been produced  
498 (Figure 26 and Figure 27 respectively). As a method with a multi-scale approach, in such large areas, this damming



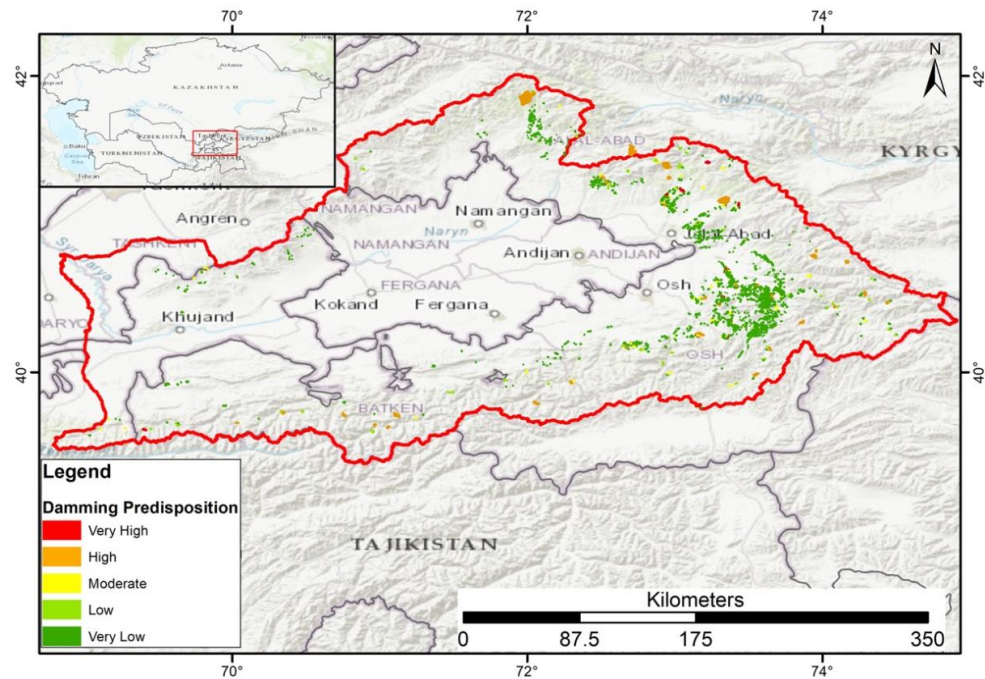
499 susceptibility method is suitable to provide territorial planning suggestions rather than indications on single  
 500 interventions at local scale. The overall damming predisposition of the Fergana valley is quite low, considering  
 501 the presence of 3370 mapped landslides in total, even if there are few landslides (10) classified with Very High  
 502 damming predisposition which should be studied with more attention through localized analysis of damming  
 503 susceptibility to ensure that downstream areas are not at risk and therefore require a specific monitoring.

504 Table 4 have been reported the distribution of the percentages of the damming susceptibility classes of those river  
 505 stretches that are not running in flat areas, since these lowland rivers represent 53.6% of the total. Concerning the  
 506 Damming Susceptibility Map of non-formation of the remaining river stretches (Figure 26), the most frequent are  
 507 Low and Moderate classes with 53.4% and 36.2% respectively, followed by Very Low class with 7.0%. Only just  
 508 2.1% and 1.3% have been classified as Very High and High. For the Damming Susceptibility Map of Formation  
 509 (Figure 27) most of the rivers fall into Very Low and Low classes with 54.5% and 38.1%, followed by Moderate  
 510 class with 5.2%. Only 1.9% and 0.2% have been classified as Very High and High respectively.

511 **Table 4. Distribution of Damming Susceptibility classes on existing landslides (Figure 25) and on the river**  
 512 **stretches for non-formation (Figure 26) and Formation of new landslides (Figure 27).**

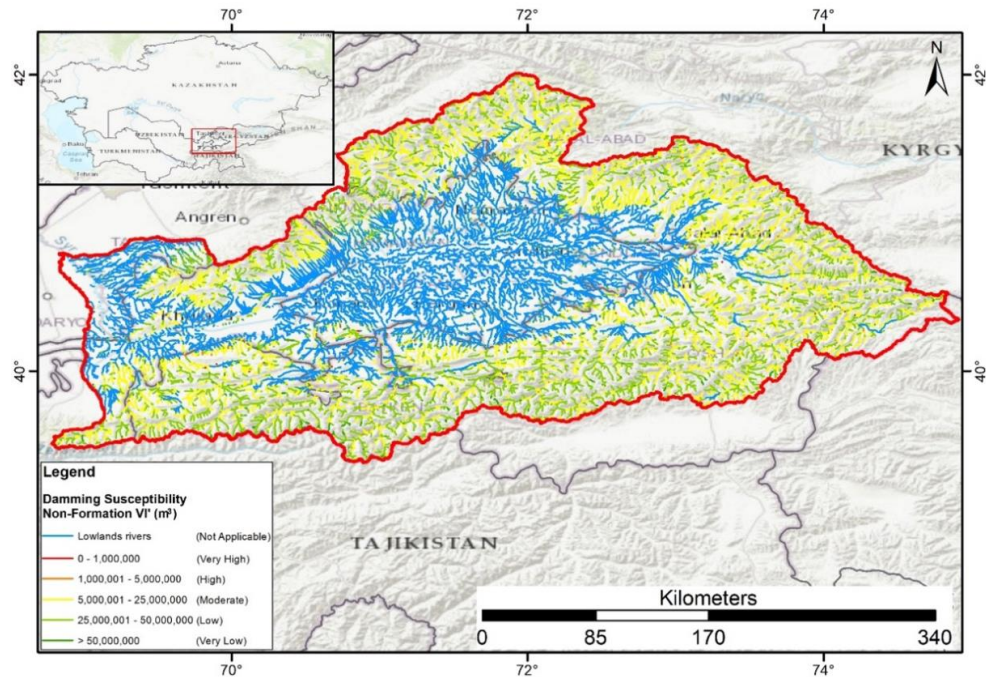
Damming Susceptibility	Landslides		non-formation	Formation
	n.	%	%	%
Very High	10	0.3%	1.9	1.7
High	48	1.4%	1.2	0.2
Moderate	61	1.8%	7.0	5.3
Low	83	2.5%	53.2	38.8
Very Low	3168	94.0%	6.7	54.0

513



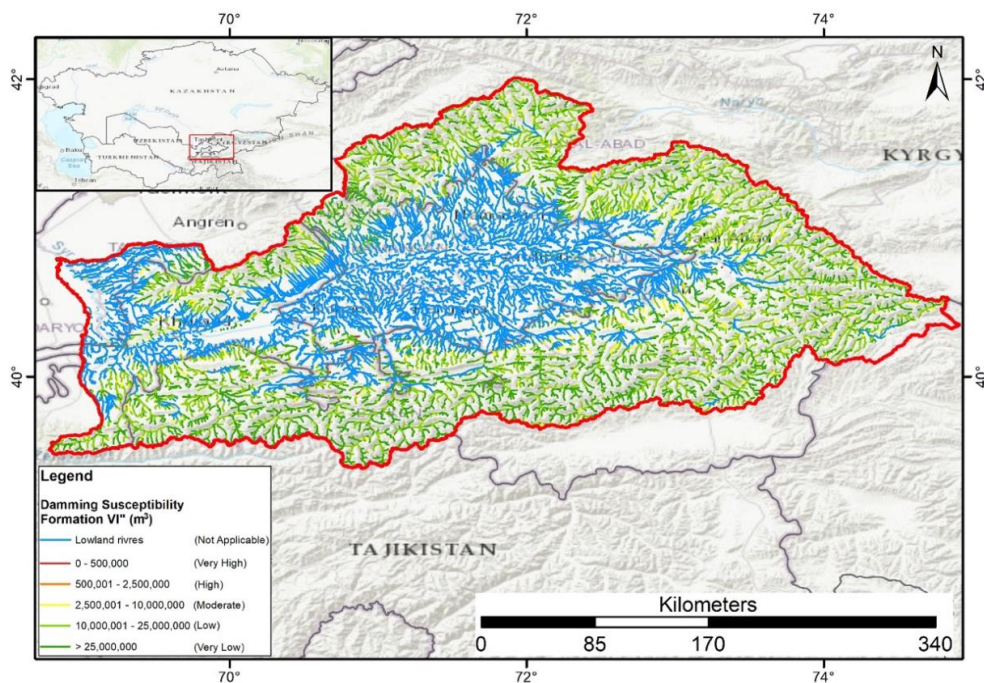
514

515 **Figure 25. Map of Damming Predisposition by landslides reactivation in the Fergana valley.** Basemap  
516 source: Esri, HERE, Garmin Intermap, increment P Corp, GEBCO, USGS, FAO, NPS, NRCAN, GeoBase, IGN,  
517 Kadaster NL, Ordnance Survey, Esri Japan, METI, Esri China (Honk Kong), © OpenStreetMap contributors,  
518 and the GIS User Community.



519

520 **Figure 26. Damming Susceptibility Map of Non-formation of river stretches by new landslides in the**  
521 **Fergana valley.** River network database from Coccia et al., (in prep.). Basemap source: Esri, HERE, Garmin  
522 Intermap, increment P Corp, GEBCO, USGS, FAO, NPS, NRCAN, GeoBase, IGN, Kadaster NL, Ordnance  
523 Survey, Esri Japan, METI, Esri China (Honk Kong), © OpenStreetMap contributors, and the GIS User  
524 Community.



525

526 **Figure 27. Damming Susceptibility Map of Formation of river stretches by new landslides in the Fergana**  
527 **valley.** River network database from Coccia et al., (in prep.). Basemap source: Esri, HERE, Garmin Intermap,  
528 increment P Corp, GEBCO, USGS, FAO, NPS, NRCAN, GeoBase, IGN, Kadaster NL, Ordnance Survey, Esri  
529 Japan, METI, Esri China (Honk Kong), © OpenStreetMap contributors, and the GIS User Community.

## 530 5 Discussion

531 During the application of the damming mapping methodology, the main issues encountered was the extremely  
532 wide study area, the amount of data and the processing time required. The used mapping methodology based on  
533 the MOI equations (Eq.(1)), was originally designed to assess the damming susceptibility at basin/regional scale  
534 (Tacconi Stefanelli et al., 2016; 2020), where the morphological parameters essential for the correct application of  
535 the tool proposed by Wood (2009) must be correctly found to have an accurate river width required in the MOI  
536 equations (Eq.(1)). This time-consuming phase has been simplified in this research, according to the wide  
537 dimension of the study area, taking into account not the basins but the different states in the Central Asia region.  
538 Furthermore, the results quality is directly proportional to the resolution and quality of the input data, which on  
539 the other hand is inversely proportional to the processing time. In this regard, a further criticality of this process is  
540 the reliability on the landslides volumes assessment method, since a higher quality of landslides data (sliding  
541 geometry and depth) allows the application of a more accurate volume calculation and therefore a better final  
542 result.



543 Thus, even if the results are not always highly reliable at local scale, requiring many in-depth specific studies in  
544 the areas identified with the higher predisposition, they can be undoubtedly useful in very large countries to adopt  
545 risk reduction measures, for planning purposes and for land development management.

546 Considering the size of the area, in Figure 10 the number of landslides classified with Very High damming  
547 predisposition (166 cases) is reasonable in absolute value, even if a bit high if compared with the total number of  
548 landslides present in the inventory (8910 cases). Without a detailed study it is not possible to say how many of  
549 these are false positives or not, however it is important to remember that this type of risk mapping methods gives  
550 information on if and where, not when these events may occur.

551 The two maps of damming susceptibility (Figure 11 and Figure 14), while not providing probability values as done  
552 by Tacconi Stefanelli et al. (2020), offer information (the volumes of landslides) that can be more easily spent and  
553 interpreted even by operators who are not specifically expert, and for this reason have more practical utility.  
554 Furthermore, the classification of the river stretches thus produced, not requiring the alpha parameter (linked to  
555 the probability of landslide occurrence) as in the original method proposed by Tacconi Stefanelli et al. (2020), it  
556 is much easier to obtain and for this reason it can be considered an improvement within a view of wider usability.

## 557 **6 Conclusions**

558 The price of a river obstruction, in terms of reconstruction and losses on both economic and lives, can be much  
559 higher compared with the costs of a proper environmental planning and land-use management. Be able to define  
560 the areas with higher risk could considerably lower the costs, allowing to focus the economic resources in effective  
561 preventive interventions, planning and monitoring activities.

562 In this work a damming mapping methodology have been proposed and carried out on the Central Asia regions.  
563 The used method, originally developed applying the Morphological Obstruction Index at basin scale, have been  
564 modified to fit such a large study area and the available data. The improvement of the original method allows a  
565 simpler use and the need for less data, more easily available, although the absence of a validation of the results  
566 inevitably remains. The main aim of this study was to propose a practical tool to assess where the damming  
567 susceptibility from reactivation of mapped landslides and formation of new landslides are higher at national scale.  
568 This second result of the mapping damming susceptibility from new landslide can be particularly useful in area of  
569 the world where there is a lack of diffuse assessment of landslide activity and incomplete landslide inventories.

570 **Code and data availability.** The landslide dam mapping susceptibility method was implemented by using the cited  
571 landslide inventory maps, published by the following authors: Behling et al., 2014, 2016, 2020; Havenith et al.,  
572 2015a; Strom and Abdrakhmatov, 2018. The SRTM DEM data are available from <https://earthexplorer.usgs.gov/>.  
573 The river network and other landslide inventories were provided by the SFRAAR project partners: RED (Risk,  
574 Engineering + Development – Pavia, Italy), OGS (National Institute of Oceanography and Experimental  
575 Geophysics, Seismological Research Center, Trieste, Italy), IWPHE (Institute of Water problems, Hydropower,  
576 Engineering and Ecology, Dushanbe, Republic of Tajikistan), ISASUZ (Institute of Seismology of the Academy  
577 of Science of Uzbekistan, Tashkent, Uzbekistan), LLP (Institute of Seismology of the Science Committee of the  
578 Republic of Kazakhstan, Almaty).



579 **Author contribution.** Carlo Tacconi Stefanelli implemented the damming mapping method, William Frodella  
580 conceived with Carlo Tacconi Stefanelli the article structure and collected the data, Francesco Caleca supported  
581 the method application on part of the study area. Francesco Caleca also performed statistical analysis involving  
582 the method results. All the aforementioned Authors contributed to the writing of the article and the figure graphics.  
583 Veronica Tofani coordinated the work and reviewed the paper. Zhanar Raimbekova and Ruslan Umuraliev  
584 provided environment and geomorphology information and part of the landslide database for Kazakhstan and  
585 Kyrgyz Republic.

586 **Competing interests.** The contact author has declared that none of the authors has any competing interests.

587 **Acknowledgements.** This work was developed within World Bank-funded project “*Strengthening Financial*  
588 *Resilience and Accelerating Risk Reduction in Central Asia*” (SFRARR), in collaboration with the European  
589 Union, and the GFDRR (Global Facility for Disaster Reduction and Recovery), with the goal of improving  
590 financial resilience and risk-informed investment planning in the central Asian countries (Kazakhstan, Kyrgyz  
591 Republic, Tajikistan, Turkmenistan and Uzbekistan). This work brings the part of the results of the Task 7  
592 “Landslide Scenario Assessment”, managed by the UNESCO Chair on Prevention and Sustainable Management  
593 of Geo-Hydrological Hazards (University of Florence, Italy). In particular, the authors would like to thank Gabriele  
594 Coccia and Paola Ceresa from Red Risk Engineering (Pavia, Italy) for providing river network data and for the  
595 valuable coordination and constant support, and also Alexander Strom and Hans Balder Havenith for providing  
596 landslide inventories and for their constructive advice and valuable observations. We would also like to thank the  
597 partners from Central Asia for the fruitful collaboration, in particular: IWPHE (Tajikistan), ISASUZ and the State  
598 Monitoring Service of the Republic of Uzbekistan for tracking dangerous geological processes (Uzbekistan), the  
599 Institute of Seismology of the National Academy of Sciences of Kyrgyz Republic (ISNASKR), and the Institute  
600 of Seismology Limited Liability Partnership (LLP) of Kazakhstan.

601 **Financial support.** This research has been supported by the World Bank Group (Consulting Services Contract No.  
602 8006611 – Regionally consistent risk assessment for earthquakes and floods and selective landslide scenario  
603 analysis for strengthening financial resilience and accelerating risk reduction in Central Asia).

#### 604 **References**

605 Abdrakhmatov, K.Y., Aldazhanov, S.A., Hager, B.H., Hamburger, M.W., Herring, T.A., Kalabaev, K.B.,  
606 Makarov, P. Molnar, S.V. Panasyuk, M.T. Prilepin, R.E. Reilinger, I.S. Sadybakasov, B.J. Souter, Yu.A.  
607 Trapeznikov, V.Ye., and Tsurkov Zubovich, A.V.: Relatively recent construction of the Tien Shan inferred  
608 from GPS measurements of present-day crustal deformation rates. *Nature*, 384(6608), 450-45319, 1996.

609 Abdrakhmatov, K., Havenith, H.B., Delvaux, D., Jongmans, D., and Trefois, P.: Probabilistic PGA and Arias  
610 Intensity Maps of Kyrgyz Republic (Central Asia). *J. Seismol.* 7.2: 203-220, 2003. Akgun, A. A comparison  
611 of landslide susceptibility maps produced by logistic regression, multi-criteria decision, and likelihood ratio  
612 methods: A case study at İzmir, Turkey. *Landslides* 2012, 9, 93–106.

613 Bazzurro, P. et al.: Strengthening Financial Resilience and Accelerating Risk Reduction in Central Asia – the  
614 SFRARR project. The SFRARR probabilistic flood hazard assessment, in preparation, 2023.





- 615 Behling, R., Roessner, S., Kaufmann, H., and Kleinschmit, B.: Automated spatiotemporal landslide mapping over  
616 large areas using rapideye time series data. *Remote Sens.* 6, 8026–8055, 2014.
- 617 Behling, R., Roessner, S., Golovko, D., and Kleinschmit, B.: Derivation of long-term spatiotemporal landslide  
618 activity—A multi-sensor time series approach. *Remote Sens. Environ.* 186, 88–104, 2016.
- 619 Behling, R., and Roessner, S.: Multi-temporal landslide inventory for a study area in Southern Kyrgyz Republic  
620 derived from RapidEye satellite time series data (2009 – 2013). V. 1.0. GFZ Data Services.  
621 <https://doi.org/10.5880/GFZ.1.4.2020.001>, 2020.
- 622 Borgatti, L., and Soldati, M.: Landslides as a geomorphological proxy for climate change: a record from the  
623 Dolomites (northern Italy), *Geomorphology*, 120(1–2), 56–64, 2010.
- 624 CAC DRMI: Risk assessment for Central Asia and Caucasus: desk study review, 2009.
- 625 Canuti, P., Casagli, N., Ermini, L., Fanti, R., and Farina, P.: Landslide activity as a geoinicator in Italy:  
626 significance and new perspectives from remote sensing, *Environ. Geol.*, 45(7), 907–919, 2004.
- 627 Casagli, N., and Ermini, L.: Geomorphic analysis of landslide dams in the Northern Apennine, *Trans. Jpn.*  
628 *Geomorphol. Union.*, 20(3), 219–249, 1999.
- 629 Catani, F., Tofani, V., and Lagomarsino, D.: Spatial patterns of landslide dimension: a tool for magnitude mapping,  
630 *Geomorphology* 273, 361–373. <https://doi.org/10.1016/j.geomorph.2016.08.032>, 2016.
- 631 Chedia, O.K., and Lemzin, I.N.: Seismogenerating faults of the Chatkal depression. In: *Seismotectonics and*  
632 *seismicity of the Tien Shan*. Frunze, Ilim, 18–28, 1980.
- 633 Coccia, G. et al.: The SFRARR probabilistic flood hazard assessment, NHESS, in preparation, 2023.
- 634 Costa, J.E., and Schuster, R.L.: Documented historical landslide dams from around the world. *US Geol. Surv.*  
635 *Open-File Report*, 91(239), 1-486, 1991.
- 636 Crozier, M.J.: Deciphering the effect of climate change on landslide activity: a review, *Geomorphology*, 124(3),  
637 260–267, 2010.
- 638 Dal Sasso, S.F., Sole, A., Pascale, S., Sdao, F., Bateman Pinzòn, A., and Medina, V.: Assessment methodology  
639 for the prediction of landslide dam hazard, *Nat. Hazards Earth Syst. Sci.*, 14 (3), 557–567,  
640 <http://dx.doi.org/10.5194/nhess-14-557-2014>, 2014.
- 641 Danneels, G., Bourdeau, C., Torgoev, I., Havenith, H. B. Geophysical investigation and dynamic modelling of  
642 unstable slopes: case-study of Kainama (Kyrgyzstan). *Geophys. J. Int.*, 175(1), 17-34, 2008.
- 643 Delvaux, D., Abdрахmatov, K.E., Lemzin, I.N., and Strom, A.L.: Landslides and surface breaks of the 1911 Ms  
644 8.2 Kemin earthquake, Kyrgyzstan, *Russian Geology and Geophysics*, 2001, 42, 10, 1667-1677, 2001.
- 645 Dikau, R., and Schrott, L.: The temporal stability and activity of landslides in Europe with respect to climatic  
646 change (TESLEC): main objectives and results, *Geomorphology*, 30(1–2), 1–12, 1999.



- 647 Drăguț, L., and Dornik, A.: Land-surface segmentation as a method to create strata for spatial sampling and its  
648 potential for digital soil mapping, *Int. J. Geogr. Inf. Sci.*, 30(7), 1359-1376, 2016.
- 649 Fan, X., Rossiter, D.G., van Westen, C.J., Xu, Q., and Görüm, T.: Empirical prediction of coseismic landslide dam  
650 formation, *Earth. Surf. Proc. Land.*, 39(14), 1913–1926, 2014.
- 651 Fan, X., Dufresne, A., Subramanian, S.S., Strom, A., Hermanns, R., Tacconi Stefanelli, C., Hewitt, K., Yunus,  
652 A.P., Dunning, S., Capra, L., Geertsema, M., Miller, B., Casagli, N., Jansen, J.D., and Xu, Q.: The formation  
653 and impact of landslide dams – State of the art, *Earth Sci. Rev.*, 203, 103116,  
654 <https://doi.org/10.1016/j.earscirev.2020.103116>, 2020.
- 655 Fan, X., Dufresne, A., Whiteley, J., Yunus, A. P., Subramanian, S.S., Okeke, C. A., Pánek, T., Hermanns, R.,  
656 Ming, P., Strom, A., Havenith, H.-B., Dunning, S., Wang, G., and Tacconi Stefanelli, C.: Recent  
657 technological and methodological advances for the investigation of landslide dams, *Earth-Sci. Rev.*, 218,  
658 103646, <https://doi.org/10.1016/j.earscirev.2021.103646>, 2021.
- 659 Farr, T.G., and Kobrick, M.: Shuttle Radar Topography Mission produces a wealth of data. *Eos Trans. AGU*, 81,  
660 583-583, 2000.
- 661 Golovko, D., Roessner, S., Behling, R., Wetzel, H. U., and Kleinschmidt, B.: Development of multi-temporal  
662 landslide inventory information system for southern Kyrgyz Republic using GIS and satellite remote sensing,  
663 *PFG*, 2015(2), 157–172, 2015.
- 664 Guzzetti, F., Ardizzone, F., Cardinali, M., Rossi, M., and Valigi, D.: Landslide volumes and landslide mobilization  
665 rates in Umbria, central Italy, *EPSL*, 279, 222–229, 2009.
- 666 Havenith, H.B., Strom, A., Cacerez, F., and Pirard, E.: Analysis of landslide susceptibility in the Suusamyr region,  
667 Tien Shan: statistical and geotechnical approach. *Landslides* 3, 39–50, 2006a.
- 668 Havenith, H.B., Torgoev, I., Meleshko, A., Alioshin, Y., Torgoev, A., and Danneels, G.: Landslides in the Mailuu-  
669 Suu Valley, Kyrgyz Republic—hazards and impacts, *Landslides*, 3, 137–147, 2006b.
- 670 Havenith, H.B., Strom, A., Torgoev, I., Torgoev, A., Lamair, L., Ischuk, A., and Abdrakhmatov, K.: Tien Shan  
671 geohazards database: Earthquakes and landslides, *Geomorphology*, 249, 16–31, 2015a.
- 672 Havenith, H.B., Torgoev, A., Schlögel, R., Braun, A., Torgoev, I., and Ischuk, A.: Tien Shan geohazards database:  
673 Landslide susceptibility analysis, *Geomorphology*, 249, 32–43, 2015b.
- 674 Havenith, H.B., Umaraliev, R., Schlögel, R., Torgoev, I., Ruslan, U., Schlogel, R., and Torgoev, I.: Past and  
675 Potential Future Socioeconomic Impacts of Environmental Hazards in Kyrgyz Republic. In *Kyrgyz Republic:  
676 Political, Economic and Social Issues*; Olivier, A.P., Ed.; Nova Science Publishers, Inc.: Hauppauge, NY,  
677 USA; pp. 63–113, 2017.
- 678 Hungr, O., and Evans, S.G.: Entrainment of debris in rock avalanches: an analysis of a long run-out mechanism,  
679 *Geol. Soc. Am. Bull.*, 116(9-10), 1240-1252, 2004.



- 680 Kalmetieva, Z.A., Mikolaichuk, A.V., Moldobekov, B.D., Meleshko, A. V., Janaev, M.M., and Zubovich, A.V.:  
681 Atlas of earthquakes in Kyrgyz Republic. Central-Asian Institute for Applied Geosciences and United  
682 Nations International Strategy for Disaster Reduction Secretariat Office in Central Asia, Bishkek, p 75, 2009.
- 683 Liao, H. M., Yang, X. G., Lu, G. D., Tao, J., and Zhou, J. W.: A geotechnical index for landslide dam stability  
684 assessment, *Geomatics, Natural Hazards and Risk*, 13(1), 854-876,  
685 <https://doi.org/10.1080/19475705.2022.2048906>, 2022.
- 686 Maxwell, A.E., and Shobe, C.M.: Land-surface parameters for spatial predictive mapping and modeling, *Earth-*  
687 *Sci. Rev.*, 226, 103944, 2022.
- 688 Molnar, P., and Tapponnier, P.: Cenozoic Tectonics of Asia: Effects of a Continental Collision: Features of recent  
689 continental tectonics in Asia can be interpreted as results of the India-Eurasia collision. *science*, 189(4201),  
690 419-426, 1975.
- 691 Niyazov R.A.: Uzbekistan landslides. Uzbekistan landslide service. Technical report, 2020.
- 692 Petrov, M.A., Sabitov, T.Y., Tomashevskaya, I.G., Glazirin, G.E., Chernomorets, S.S., Savernyuk, E.A.,  
693 Tutubalina O.V., Petrakov, D.A., Sokolov, L.S., Dokukin, M.D., Mountrakis, G., Ruiz-Villanueva, V., and  
694 Stoffel, M.: Glacial lake inventory and lake outburst potential in Uzbekistan, *Sci. Total Environ.*, 592, 228-  
695 242, 2017.
- 696 Piroton, V., Schlögel, R., Barbier, C., and Havenith, H.B.: Monitoring the recent activity of landslides in the  
697 Mailuu-suuy valley (Kyrgyz Republic) using radar and optical remote sensing techniques. *Geosciences*, 10  
698 (5), p. 164, 2020.
- 699 Popescu, M.E., and Sasahara, K.: Engineering Measures for Landslide Disaster Mitigation, in: *Landslides –*  
700 *Disaster Risk Reduction*, edited by: Sassa, K., Canuti, P., Springer, Berlin, Heidelberg, 609-631,  
701 [https://doi.org/10.1007/978-3-540-69970-5\\_32](https://doi.org/10.1007/978-3-540-69970-5_32), 2009.
- 702 Righini, M., and Surian, N.: Remote sensing as a tool for analysing channel dynamics and geomorphic effects of  
703 floods, *Flood monitoring through remote sensing*, 27-59, 2018.
- 704 Rosi, A., Frodella, W., Nocentini, N., Caleca, F., Havenith, H.B., Strom, A., Saidov, M., Bimurzaev, G.A., and  
705 Tofani, V.: Comprehensive landslide susceptibility map of Central Asia, *Nat. Hazards Earth Syst. Sci.*, 23,  
706 2229–2250, <https://doi.org/10.5194/nhess-23-2229-2023>, 2023.
- 707 Saponaro, A., Pilz, M., Wieland, M., Bindi, D., Moldobekov, B., and Parolai, S.: Landslide susceptibility analysis  
708 in data-scarce regions: the case of Kyrgyz Republic. *Bull. Eng. Geol. Environ.* 74, 1117–1136, 2014.
- 709 Schlögel, R., Torgoev, I., De, Marneffe, C., and Havenith, H.B.: Evidence of a changing size-frequency  
710 distribution of landslides in the Kyrgyz Tien Shan, Central Asia. *Earth Surf Process Landf* 36(12), 1658–  
711 1669, 2011.
- 712 Schuster, R.L., and Evans, S.G.: Engineering Measures for the Hazard Reduction of Landslide Dams, in: *Natural*  
713 *and Artificial Rockslide Dams. Lecture Notes in Earth Sciences*, edited by: Evans, S., Hermanns, R., Strom,



- 714 A., Scarascia-Mugnozza, G., Springer, Berlin, Heidelberg, [https://doi.org/10.1007/978-3-642-04764-0\\_2](https://doi.org/10.1007/978-3-642-04764-0_2),  
715 2011.
- 716 Semakova, E., Gunasekara, K., and Semakov, D.: Identification of the glaciers and mountain naturally dammed  
717 lakes in the Pskem, the Kashkadarya and the Surhandarya River basins, Uzbekistan, using ALOS satellite  
718 data, *Geomat. Nat. Hazards Risk*, 7(3), 1081-1098, 2016.
- 719 Strom, A.: Landslide dams in Central Asia region. *Journal of the Japan Landslide Society*, 47(6), 309-324, 2010.
- 720 Strom, A., and Abdrakhmatov, K.: Large-Scale Rockslide Inventories: From the Kokomeren River Basin to the  
721 Entire Central Asia Region (WCoE 2014–2017, IPL-106-2, in: Workshop on World Landslide Forum.  
722 Springer, Cham, pp. 339–346, 2017.
- 723 Strom, A., and Abdrakhmatov, K.: Rockslides and rock avalanches of Central Asia: distribution, morphology, and  
724 internal structure. Elsevier, 441pg. ISBN: 978-0-12-803204-6, 2018.
- 725 Swanson, F.J., Oyagi, N., and Tominaga, M.: Landslide dams in Japan, in: *Landslide dams: processes, risk and  
726 mitigation*, vol 3, edited by: Schuster R.L., Geotech. Sp., ASCE, New York, 131–145, 1986.
- 727 Tacconi Stefanelli, C., Segoni, S., Casagli, N., and Catani, F.: Geomorphic indexing of landslide dams evolution,  
728 *Eng. Geol.*, 208, 1–10. <https://doi.org/10.1016/j.enggeo.2016.04.024>, 2016.
- 729 Tacconi Stefanelli, C., Vilímek, V., Emmer, A., and Catani, F.: Morphological analysis and features of the  
730 landslide dams in the Cordillera Blanca, Peru, *Landslides*, 15(3), 507-521, [https://doi.org/10.1007/s10346-  
731 017-0909-5](https://doi.org/10.1007/s10346-017-0909-5), 2018.
- 732 Tacconi Stefanelli, C., Casagli, N., and Catani, F.: Landslide damming hazard susceptibility maps: a new GIS-  
733 based procedure for risk management, *Landslides*, 17, 1635-1648, [https://doi.org/10.1007/s10346-020-  
734 01395-6](https://doi.org/10.1007/s10346-020-01395-6), 2020.
- 735 Trifonov, V.G., Makarov, V.I., and Scobelev, S.F.: The Talas-Fergana active right-slip faults. *Ann Tectonicae*  
736 6:224–237, 1992.
- 737 Ullah, S., Bindi, D., Pilz, M., Danciu, L., Weatherill, G., Zuccolo, E., Anatoly Ischuk, A., Mikhailova, N.N.,  
738 Abdrakhmatov, K., and Parolai, S. Probabilistic seismic hazard assessment for Central Asia. *Annals of  
739 Geophysics*, 58(1), 2015.
- 740 Wang, X., Ding, Y., Liu, S., Jiang, L., Wu, K., Jiang, Z., and Guo, W.: Changes of glacial lakes and implications  
741 in Tian Shan, central Asia, based on remote sensing data from 1990 to 2010, *Environ. Res. Lett.*, 8(4),  
742 044052, 2013.
- 743 Wang, D., Laffan, S.W., Liu, Y., and Wu, L.: Morphometric characterization of landform from DEMs, *Int. J.  
744 Geogr. Inf. Sci.*, 24(2), 305–326, 2010.
- 745 Wood, J.: Geomorphometry in LandSerf. In: Hengl, T. and Reuter, H.I. [Eds.]: *Geomorphometry: Concepts,  
746 Software, Applications, Dev. Soil. Sci.*, 33, 333-349, 2009.



747 Zubovich, A. V., Wang, X. Q., Scherba, Y. G., Schelochkov, G. G., Reilinger, R., Reigber, C., Mosienko, O.,  
748 Molnar, P., Michajljow, W., Makarov, V.I., Li, J., Kuzikov, S.I., Herring, T.A., Hamburger, M.W., Hager  
749 B.H., Dang, Y., Bragin, V.D., and Beisenbaev, R.: GPS velocity field for the Tien Shan and surrounding  
750 regions. *Tectonics*, 29(6), 2010.